JPL D-5698

Distribution Category
UC-93

ECUT
Energy Conversion and Utilization Technologies Program

Direct Conversion Technology

Annual Summary Report CY 1988

JPL-D--5698

DE89 003911

Prepared by:

Paul F. Massier
and by
C. P. Bankston and G. Fabris
Jet Propulsion Laboratory
California Institute of Technology
and by
L. D. Kirol
EG & G Idaho, Inc.

December 1, 1988

Sponsored by

Energy Conversion and Utilization Technologies Program
Office of Energy Utilization Research
U.S. Department of Energy
Washington, D.C. 20585

Through an agreement with

National Aeronautics and
Space Administration

by

Jet Propulsion Laboratory
California Institute of Technology
Pasadena, California

Prepared by the Jet Propulsion Laboratory, California Institute of Technology, for the U.S. Department of Energy through an agreement with the National Aeronautics and Space Administration.

The work reported herein was performed through NASA Task RE-152, Amendment 308, and was sponsored by the United States Department of Energy under IAA DE-AI01-86CE90237.

TABLE OF CONTENTS

LIST OF TABLES AND FIGURES

SUMMARY

The overall objective of the Direct Conversion Technology task is to develop an experimentally verified technology base for promising direct thermal-to-electric energy conversion systems that have potential application for energy conservation in the end-use sectors.

This report contains progress of research on the Alkali Metal Thermal-to-Electric Converter (AMTEC), and on the Two-Phase Liquid-Metal MHD Electrical Generator (LMMHD) for the period January 1988 through December 1988. Research on these concepts was initiated during October 1987. In addition, status reviews and assessments are presented for thermomagnetic converter concepts and for thermoelastic converters (Nitinol heat engines). Reports prepared on previous occasions (Refs. 1 and 2) contain discussions on the following other direct conversion concepts: thermoelectric, pyroelectric, thermionic thermophotovoltaic and thermoacoustic; and also, more complete discussions of AMTEC and LMMHD systems. A tabulated summary of the various systems which have been reviewed thus far has been prepared. Some of the important technical research needs are listed and a schematic of each system is shown. These tabulations are included herein as figures.

The 2nd U.S. **Alkali Metal Thermal-to-Electric Converter (AMTEC)** workshop was held at JPL on March 10 and 11, 1988. The meeting was attended by over 40 representatives of 18 industrial and government organizations. Presentations covered all known work on AMTEC technology in the U.S., Canada and Japan. Two important conclusions relevant to ECUT/AMTEC work at JPL were: 1) JPL's modeling capabilities were recognized as important for the prediction of AMTEC performance in real systems and it was recommended that these capabilities continue to be expanded: and 2) there is a strong need for new experimental thermal analysis and efficiency data on self-contained recirculating devices. Work in both of these areas is contained in the ECUT plan.

Mr. Robert K. Sievers, Staff Engineer, Westinghouse Advanced Energy Systems Division, Pittsburgh, joined Caltech/JPL as a visiting industry associate in September 1987 and remained through September 1988. This is in

connection with Mr. Sievers being awarded the Westinghouse Lamme Scholarship for one year of academic work and independent study. Westinghouse has previously investigated AMTEC technology for space nuclear power applications for DOE, and presently is exploring several potential markets for AMTEC commercialization (in addition to space nuclear power).

Several experiments on very thin molybdenum electrodes with grids were carried out by JPL researchers in the electrode test cell. In one experiment, one electrode was still producing 0.44W/cm^2 at 1110°K after 160 hours at temperatures above 1000°K. In another experiment, one electrode produced 0.47W/cm^2 after 100 hours at high temperature. These experiments are the best performance yet observed for this class of electrodes. Model predictions now indicate that 0.6W/cm^2 should be available from these electrodes, which would result in AMTEC device efficiencies of at least 20%. Contact resistances have been identified as the principal factor that has limited power densities to about 0.5W/cm^2 to date. Means to optimize contacts are being investigated.

In addition, several experiments on platinum-group/tungsten electrodes were also carried out and it has been shown that this group now repeatedly performs in the 0.5-0.8 W/cm^2 range. Power densities at 0.7-0.8 W/cm^2 are higher than any other stable power densities ever measured at any time in AMTEC devices. Detailed modeling of the AMTEC electrode has been completed and a new current versus voltage expression for these electrodes has recently been derived.

Research on the **Two-Phase Liquid-Metal MHD Electrical Generator** is focused on the reduction of slip between the gas bubbles and the liquid metal during the expansion process in the MHD electrical generator. Air and water mixes with the addition of surface active agents (surfactants) are being investigated to determine the factors that control mixture uniformity and prevention of bubble coalescence. A facility for doing this has been set up and experiments are in progress. The knowledge gained from these experiments is being used to design and construct the mixing section of a liquid-metal generator blowdown system which will be used for conducting experiments with actual system working fluids such as NaK.

Thermomagnetic Generator Concepts have been reviewed. Some of these systems can convert thermal energy directly into electrical energy, without a mechanical interface, by appropriate utilization of the caloric effect of solid ferromagnetic materials. At or near the Curie temperature of such materials large changes of magnetization (alignment of magnetic dipoles) occur over relatively small temperature changes even in the absence of an applied magnetic field, but more dramatically in the presence of externally applied fields. Associated with these temperature and magnetization changes there are also changes in entropy. These phenomena have previously been used to construct thermodynamic cycles for heat engines, refrigerators, and electrical generators.

Systems have been conceived in which a shunt of solid ferromagnetic material is placed in the air gap between the pole pieces of a stationary magnet. An electrically conducting coil surrounds the shunt and the magnetic flux lines of the magnet. The temperature of the shunt material is then cycled by heating and cooling. Changes in the temperature of the shunt material span the Curie point and hence, produce changes in the magnetic flux. This induces voltage in the coil and as a result, a current will flow.

Another version consists of a toroid made of a solid ferromagnetic material which during part of its circumferential travel rotates through an applied magnetic field region. The segment of the toroid which is inside the magnetic field at anytime is being heated; whereas, that part which is outside the bounds of the field is simultaneously being cooled. The cold side, because of its higher magnetization, is attracted into the applied field region, and as a consequence, torque is generated which produces a continuous rotation. Hence, either electrical power or mechanical shaft power is generated.

Active magnetic regenerative systems have also been conceived in which ferromagnetic materials of descending Curie temperatures are staged, for example, in a wheel or disk arrangement, so that larger temperature ranges can be accommodated in a single system. Previous analytical work on these devices has been focused on refrigeration. These analyses should be extended to apply

Still another thermomagnetic version is based on the utilization of a suspension of very fine (less than 100 angstroms) particles of a ferromagnetic material in a carrier fluid which is the working substance. This colloidal suspension (ferrofluid) is circulated through a system where it is heated as it passes through a combined solenoid and heat exchanger. Then it is cooled to increase its magnetization, and after that it flows through a magnetohydrodynamic generator where electrical power is produced. The fluid then returns to the solenoid and is recycled in the system.

Some analyses of these various concepts have been performed; however, considerably more effort in this regard is needed. Also, experimental performance information does not appear to exist; hence, experimental verification of these systems is needed.

Thermoelastic Converters (Nitinol Engine) have also been reviewed. These systems are based on the use of metal alloys that possess a unique mechanical shape "memory" property. Nitinol is the generic name for a range of these alloys which consist of nickel and titanium. The "memory" effect is a consequence of a solid-solid phase transformation from a martensitic phase to a parent austenitic phase when the material is heated to a critical transition temperature. A specimen of Nitinol may be elastically deformed at a temperature below the alloy's transition temperature by applying a load at a moderately low stress. Then, if the temperature of the specimen is raised above the transition point, the specimen will recover ("snap back" to) its earlier shape. The forces exerted by the specimen during the hotter recovery process can greatly exceed those required during deformation and may be as much as 200 times greater than those exerted by bimetals. Therefore, the specimen has the ability to perform mechanical work from heat input. The transition temperature can be manipulated over a remarkably wide range from about -459°F to 212°F (-273°C to 100°C) by altering the nickel-titanium ratio and by adding small amounts of other elements. Based on these properties of Nitinol, researchers have conceived and built various configurations of small heat engines that operate over comparatively small temperature differences. Hence, with acceptable performance and cost they would be suitable for waste heat

energy conversion. The next phase of Nitinol heat engine development should consist of design, construction, and testing of a prototype for a particular application. A method of utilizing the properties of Nitinol in a direct thermal-to-electrical energy conversion mode without a mechanical interface, however, has, as yet, not been conceived.

A. INTRODUCTION

During 1984 the estimated energy consumption in the United States by the combined industrial, commercial, residential, and transportation sectors was about 72 quads (1 quad = 10^{15} BTU) and, for example, approximately 75% of the energy used in the United States by our ten most energy intensive industries is used in heating or conversion processes. In general, these energy conversion processes are not as efficient as possible, because a substantial percentage of the input energy is rejected as waste heat. The main driver for justifying rejection is that economical systems for conversion of this wasted thermal energy into a more useful form such as electricity (which is easy to transport) do not exist. Most of this wasted heat is at temperatures below about 250°C. Figure 1 shows the relative amounts of thermal energy that are wasted in industrial streams of temperatures between 30°C and 290°C. This information was developed by Olsen (Ref. 3) and was taken from the data given in Table 1 of Ref. 4. As might be expected, more energy is wasted at the lower temperatures. Hence, direct conversion of waste heat energy to electricity can be an important component in energy conservation efforts. Applications for the utilization of industrial waste heat directly (without conversion) via hot water streams for residential heating have been explored (cf. Ref. 4). In Europe the use of centrally located thermal plants set up to supply hot water for residential heating has apparently been successful in large residential development areas. The load requirements for such heating are seasonal being dependent on the weather. Hence, if industrial streams were used for this purpose, during extended periods of minimum or no load requirements it would still be necessary for industrial plants to reject much of their waste heat.

Although the conversion of waste heat to electricity is an important application for direct conversion systems, some concepts are suitable only for operation at much higher heat source temperatures. Topping cycle and cogeneration applications are also important for overall systems in which direct conversion concepts will enhance performance. A broad range of techniques exist for direct conversion; however, none have been reduced to the level of practice required for cost-effective energy conservation applications. Hence, research is needed to advance a technology base which would be in demand

for application by the end-use sectors. Furthermore, the main focus should be on cross-cutting technologies because approximately 1/3 of the 72 quads represents energy used for which the technological phenomena are common to all sectors.

What appears to be a shortcoming of low-temperature direct-conversion systems is their inherent low thermal efficiency. A better performance parameter, however, is the percent of Carnot efficiency which any given system will produce. The highest attainable efficiency, which is Carnot, is dependent on temperature difference between the heat input and heat rejection temperatures, and on the absolute temperature of the heat source. Figure 2 shows the variation of Carnot efficiency with these temperatures, and the high rate of change, particularly at the low end of the temperature scale. Hence, a system which may be as high as 60% of Carnot, may at a very low heat input temperature, still only have a thermal efficiency of a few percent. **However, it is important to note that any conversion system which produces energy at a cost less than the prevailing rates will be economically viable, independent of efficiency, or any other purely technical criterion.**

During CY 1986 an assessment was made to establish some of the most promising direct conversion systems (Ref. 1). Performance status relative to projected performance was established and research needs for promising technologies were identified. Screening was based on stage of development, ease of implementation, projected and demonstrated thermal-to-electric energy-conversion efficiency, and broadness of potential applicability. Out of this group the alkali metal thermal-to-electric converter (AMTEC) and the two-phase liquid-metal MHD generator (LMMHD) were selected for support by ECUT beginning in CY 1987. This report covers the recent progress that has been made on AMTEC and LMMHD research, and on the evaluation of thermomagnetic and thermoelastic systems. These latter two systems had not been assessed for ECUT previously. The identification and assessment of other concepts is being continued.

B. OBJECTIVES

The overall objective of the direct conversion technology task is to develop an experimentally verified technology base for promising direct thermal-to-electric conversion systems that have potential application for energy conservation in the end-use sectors. Specific objectives are:

1. For the Alkali Metal Thermal-to-Electric Converter continue the research to increase the lifetime of electrodes by investigating the most promising materials, which consist of molybdenum and its alloys, and continue detailed thermal analysis of the AMTEC cycle.

2. For the Two-Phase Liquid-Metal MHD Electrical Generator continue the research to improve the performance of the generator by exploring methods to reduce slip between the expanding gas bubbles and the liquid metal.

3. Continue to examine advanced and innovative direct thermal-to-electric energy conversion concepts, identify those that are promising, determine industrial needs for application, which concept should be used for which industrial need, and determine critical research needs for promising concepts.

C. TABULATED SUMMARY OF ALL REVIEWED CONCEPTS

The various thermal-to-electric energy conversion concepts that have been reviewed thus far as part of the assessment activity are summarized in Figs. 3 through 8. Each concept is identified, some of the important technical research needs are listed, and a schematic of each system is shown. A few of these systems are not direct conversion in the configurations shown; however, most might possibly be modified in some way such that a mechanical interface between an output shaft and an additional conventional generator would not be needed, particularly the rotary thermomagnetic devices that require an applied magnetic field as an essential component of the system to make it operable. The thermoelastic (nitinol engine) converter is included because its operation

is feasible at hot water temperatures and over small temperature differences which makes it suitable for converting the thermal energy in industrial waste heat streams to mechanical and electrical energy.

The combined thermomagnetic with pyroelectric system of Fig. 8 is merely in a state of suggestion. As yet there is no known analysis or proposed system arrangement for this combination; however, it should be analyzed at some point.

The listings in Figs. 3 through 8 are not in any prioritized sequence. True priortization requires input of more specific industrial applications and industrial needs. Such studies have not yet been completed. In the interim, however, it appears that the more promising concepts for ECUT to pursue from a technical standpoint are some of the thermomagnetic systems. This conclusion, however, excludes those converters such as thermionic and thermoelectric which have received substantial funding from other sources over a period of many years, and as a consequence, are in a more advanced state of development even though ideas for improvements that require research have been brought forth.

D. RESEARCH ACTIVITIES

1. Alkali Metal Thermal-to-Electric Converter (AMTEC)

The 2nd U.S. AMTEC Workshop was held at JPL on March 10 and 11, 1988. (The first one was held on April 24 and 25, 1986, also at JPL.) The meeting was attended by over 40 representatives of 18 industrial and government organizations. Presentations covered all known work on AMTEC technology in the U.S., Canada and Japan. Two important conclusions relevant to ECUT/AMTEC work at JPL were: 1) JPL's modeling capabilities were recognized as important for the prediction of AMTEC performance in real systems and it was recommended tnat these capabilities continue to be expanded, and 2) there is a strong need for new experimental thermal analysis and efficiency data on self-contained recirculating devices. Work in both of these areas is contained in the ECUT plan.

Mr. Robert K. Sievers, Staff Engineer, Westinghouse Advanced Energy Systems Division, Pittsburgh, joined Caltech/JPL as a visiting industry associate in September 1987 and remained through September 1988. This is in connection with Mr. Sievers being awarded the Westinghouse Lamme Scholarship for one year of academic work and independent study. Westinghouse has previously investigated AMTEC technology for space nuclear power applications for DOE.

Upon his selection as a Lamme Scholar, Mr. Sievers, in consultation with Westinghouse management, asked if he could serve the year at JPL to learn AMTEC technology while taking courses at Caltech. Mr. Sievers worked approximately one-half time in the AMTEC laboratory while taking Caltech courses. He contributed to both experimental and systems studies of AMTEC technology. Presently, Westinghouse is exploring several potential markets for AMTEC commercialization (in addition to space nuclear power) and the expertise obtained by Mr. Sievers would be directly applicable to any subsequent AMTEC development at Westinghouse.

Several experiments on very thin molybdenum (VTM) electrodes with grids were carried out by JPL researchers in the electrode test cell. A summary of the performance of these electrodes is given in Fig. 9. Note that one electrode was still producing o.44W/cm^2 at 1110°K after 160 hours at temperatures above 1000°K. In another experiment, one electrode produced 0.47W/cm^2 after 100 hours at high temperature. These experiments are the best performance yet observed for this class of electrodes. Model predictions now indicate that 0.6W/cm^2 should be available from these electrodes, which would result in AMTEC device efficiencies of at least 20%. Contact resistances have been identified as the principal factor that has limited power densities to about 0.5W/cm^2 to date. Means to optimize contacts are being investigated.

In addition, several experiments on platinum-group/tungsten electrodes were also carried out in the electrode test cell. A summary of the performance of these electrodes is given in Fig. 10. The results show that platinum-group/tungsten electrodes now repeatedly perform in the 0.5-0.8 W/cm^2 range. Power densities at 0.7-0.8 W/cm^2 are higher than any other stable power

densities ever measured at any time in AMTEC devices. The ability to repeat this performance, as shown, is a major accomplishment of this year's research, and device efficiencies of 20% or greater appear certain if lifetimes of 1000 hours or more are demonstrated. The very high power electrodes (rhodium or platinum with tungsten) are 1-3 μm thick with compositions of more than 50% noble metal. Rhodium is expected to be somewhat more stable for very long lifetimes, since rhodium is more refractory than platinum. Correlation of morphology with deposition conditions and performance is now being carried out so that deposition conditions can be routinely specified for high power operation.

Detailed modeling of the AMTEC electrode has been completed and a new current versus voltage expression for these electrodes has recently been derived (Ref's. 5 and 6). The new expression is based on the electrochemical current overpotential equation.
Current density, j, is given in A/cm^2, by:

$$j = j_0(\exp[-\alpha\eta f] - [(P_j + P\Delta + P_l)/P_l] \exp[(1 - \alpha)\eta f])$$

The cell voltage V, is contained in the definition of:

$$\eta = V - E_{oc} + jR_{TO},$$

R_{TO} is the total ohmic resistance and E_{oc} is the open circuit voltage. P_j is the pressure due to sodium leaving the electrode, $P\Delta$ is the sodium vapor pressure drop within the pore, and P_l is the sodium pressure due to evaporation at the condenser. $f = F/(RT_2)$, where F is Faraday's constant, and R is the gas constant, j_0 is the exchange current density at E_{oc}, and α is the electrochemical transfer coefficient. j_0 and α are determined from curve fits to measured charge transfer resistance data. Calculations of cell current versus voltage expressions are then carried out using finite elements and integrating over the electrode surface among current collector grid elements.

Previously, the model included transport loss through the electrode pores ($P\Delta$) but lumped other loss mechanisms into the total ohmic resistance to fit

the data. This new formulation takes into account possible kinetic limitations by including the parameters j_0 and α, and now more accurately characterizes electrode processes. A curve fit of the data (points) for an Rh/W electrode is shown in Figure 11. In this figure the cell voltage is plotted versus the current density of the electrode for four different electrodes fabricated the same way. A significantly higher series resistance R_S, is apparent for the electrode designated as E4 than for the others. The performance of this electrode shows a comparative rapid decrease in voltage with current density. The rate of decrease for the other electrodes is not as large. Series resistance includes the sum of the ionic resistance of sodium through the β" alumina, the sheet resistance in the electrode and grid, and the contact resistances between the collection wire and grid, as well as between the grid and the sheet. All of these tests were conducted at a hot sodium temperature T_2 of roughly 1200°K. The value of G is $\ell \div (a^3 n)$, where ℓ is the electrode thickness, a is the radius of the pores and n is the number of pores per unit area. The value of G, when in the range of about 10 to 30 has been found not to affect the results. Accurate modeling of electrode performance will allow device performance characteristics to be confidently predicted for a wider range of temperatures than can now be simulated in the laboratory.

Finally, an electromagnetic pump for the recirculating test cell (RTC) was successfully tested. It achieved 30 psi pumping pressure, which is more than adequate for maintaining sodium recirculation. The RTC has also undergone some minor modifications and thermal testing. In thermal testing, the cell was heated to operating temperatures, first without sodium and then with sodium in the vacuum space. The temperatures at various points of the condenser and heater well were measured as a function of input power. A simple computer model was developed to analyze these inputs and determine the primary heat loss mechanisms and the effectiveness of the radiative heat transfer within the cell. A smooth film of reflective sodium was achieved on the condenser wall and initial calculations show the reflectivity to be greater than 95%. The RTC is now being readied for resumption of operation.

A paper titled "Progress in AMTEC Electrode Experiments and Modeling"

(Ref. 5) was presented at the 23rd Intersociety Energy Conversion Engineering Conference held in Denver, Colorado, July 31 to August 5, 1988.

2. Two-Phase Liquid-Metal MHD Electrical Generator (LMMHD)

Efficient generation of electricity in the two-phase liquid-metal MHD generator concept requires that small bubbles of gas be well mixed with the liquid metal during the time that this mixture expands to a lower pressure in the generator. The expanding gas bubbles "push" the surrounding liquid against the Lorentz force which results from the interaction of the electrically conducting liquid metal with an applied magnetic field. A focus of the present research is to develop and understand methods for reducing slip between the expanding gas bubbles and the liquid metal. A more detailed discussion of the system concept and of the expansion process appears in Ref. 1.

The approach is to first investigate the factors that control mixture uniformity by conducting designed experiments using air and water with and without the addition of surface active agents (surfactants).

A facility for performing these experiments has now been completed. Air and water mixtures are used because advancements in understanding mixing and bubble behavior can be made much more rapidly than by starting directly with a liquid metal. Visual observation is possible and the fluids are safe to use. The most critical factor in simulating the dynamics of gas/liquid metal mixing is prevention of bubble coalescence by surface activity. The formation of bubbles at a gas injection surface is governed by wetting, by buoyancy, and by fluid dynamic drag forces on the bubbles. Use of surface active additives ensures good wetting; however, different additives would be used in the liquid metal system than in water so as to avoid reactions. The buoyancy and drag forces are influenced primarily by density and viscosity. Both density and viscosity of sodium-potassium (NaK) are only 15 percent smaller than corresponding values for water. A significantly higher pressure will exist in the NaK-N_2 system which means that the density of the gas will be different; however, the density of the gas plays a negligible role in the bubble flow mixing process.

Figure 12 shows a schematic of the system. The water, metered by a turbine flow meter, enters at the bottom of the test section and flows vertically upward. Compressed air at a few psig enters the mixing test section through the injection element. Injection of the surfactant into the water occurs sufficiently upstream of the test section to obtain homogeneous mixing. Surfactant metering will be carried out by timing the lowering of the level of surfactant in the tank.

Figure 13 is a photograph of the air-water system which shows the vertical transparent test section at the left. Details of the test section are shown on Fig. 14. The transparent channel has a square cross section of 4 inches on a side and is 80 inches long. In the first twenty inches flow non-uniformities caused by abrupt enlargement of the cross section at the channel entrance are minimized. A perforated plate and a honeycomb are used for this purpose. The air injection element is two-dimensional with a faired trailing edge. Two wedged wall inserts start in the region of the trailing edge of the injection element. They create a favorable pressure gradient along the flow thereby preventing separation. Figure 15 is a photograph of the lower (inlet part) of the test section. The perforated plate at the bottom, the honeycomb made of closely packed soda straws, and the air injection element are plainly visible. Details of the air injection element are shown in Fig. 16 and a photograph of this is shown in Fig. 17. The large air injection area is necessary for achievement of high void fraction in the water side of the test channel. Air is introduced into the injection element through six holes along the side. A rounded leading edge and a tapered trailing edge prevent flow separation which can be a source of detaching large gas bubbles that move downstream with considerable slip velocity. Experiments are in progress.

After the air-water tests have been completed a liquid-gas mixing section will be designed and generator performance experiments will be performed in a liquid-metal blowdown system using NaK and Nitrogen. A BUX Shrader (60 volts, 55 amperes) dc electromagnet which has pole faces of 13 by 6 inches with an air gap of 6 inches will supply the magnetic field. These dimensions are sufficient for insertion of an LMMHD generator.

E. DESCRIPTIONS OF DIRECT CONVERSION CONCEPTS REVIEWED DURING CY 1988

1. Thermomagnetic Generators

The conversion of thermal-to-electrical energy by means of a thermomagnetic generator can be accomplished, without a mechanical energy interface, by appropriate utilization of the magnetocaloric effect of solid ferromagnetic materials (Ref. 7). Examples of ferromagnetic materials are iron, nickel and cobalt, but there are many others including compounds and alloys. At or near the Curie temperature of such materials large changes of magnetization occur over relatively small changes in temperature.

Since the general topic of direct conversion involves various disciplines, perhaps at this point a refresher on some of the definitions and the terminology associated with magnetism and what actually takes place when a magnetic field is applied to a system is in order. A **ferromagnetic** material is one in which the magnetic moments of atoms or ions (magnetic dipoles) tend to become aligned parallel to one another when the material is below some characteristic temperature. This takes place in the absence of an applied magnetic field, but more dramatically in the presence of externally applied fields. The characteristic (or transition) temperature is known as the **Curie point** (which is lower than the melting point). The magnetic atomic moment can also be expressed in terms of the Bohr magneton, the moment which arises from the motion of a single electron moving in its smallest orbit (Ref. 8). During the alignment process, in an adiabatic system, the magnetic entropy decreases; and since internal energy is constant, spin-lattice coupling causes the lattice entropy to increase. This combination of energy exchanges is known as the **magnetocaloric effect**. Perhaps a more understandable description of what takes place in the magnetocaloric effect is given by Hull and Uherka in Ref. 9 as follows. When a volume of material containing individual magnetons, initially oriented so that there is no net magnetization, experiences on applied magnetic field, the magnetons tend to line up with the external field. If the process is adiabatic, the energy of magnetization is transferred to the lattice as thermal energy and the material heats up. Then, when the applied field is removed from the aligned system, spin-lattice coupling transfers thermal energy

from lattice vibration to the randomization of the magnetons, and thus the lattice is cooled.

When heated above the Curie point, ferromagnetic materials become **paramagnetic**, i.e., dipole misalignment takes place and the result is that there is only partial alignment of the magnetic dipole moments. Figure 18, for example, taken from Ref. 8, shows how magnetization of iron, a ferromagnetic material, changes with temperature and with an externally applied field. The Curie temperature for iron is 770°C. The rapid change of magnetization with temperature change is apparent in the vicinity of the Curie temperature. The quantity, μ_0, is the magnetic permeability of free space. Its value in the cgs system is unity.

Magnetic processes are analogous to gas processes in heat engines, heat pumps and refrigerators. An isothermal process in a magnetic system, for example, is obtained by specifically programmed heat rejection with increase in magnetization, or programmed heat addition with demagnetization. A constant applied magnetic field process is analogous to a constant pressure gas process, and a constant magnetization (or demagnetization) process is analogous to a constant volume gas process. The difference between applied magnetic field and magnetization of the material should be noted. Application of a magnetic field is an external effect; whereas, magnetization is an internal effect. Internal changes in properties are greatest at the Curie temperature of the material.

These phenomena can be used to construct thermodynamic cycles for heat engines, refrigerators and electrical generators. They have, in fact, been used in refrigeration for many years to achieve temperatures that approach absolute zero (Refs. 10, 11, and 12).

The entropy equation associated with thermal processes in solid magnetic materials experiencing applied magnetic fields is given as (from Ref. 13)

$$dS = \frac{C_B}{T} dT + \left(\frac{\partial M}{\partial T}\right)_B dB \qquad (1)$$

The quantity S, is entropy, B is the magnetic field, C_B is heat capacity (specific heat) at constant magnetic field, M is magnetization, and T is absolute temperature. Thus, in order to predict the isothermal entropy change, or the adiabatic (isentropic) temperature change with magnetic field variation, the zero-magnetic-field heat capacity and the equation of state are required. These and other relationships together with the procedure for obtaining calculations are not given here but may be found in Ref. 13.

In order to more fully understand and appreciate the capability of magnetic systems, it is instructive to compare the thermodynamics of the magnetic system, and that of the gas system with which the reader may be more familiar. The entropy equation for a gas system (perfect gas) which corresponds to Eq. (1) is

$$dS = \frac{C_P}{T} dT - \frac{R}{P} dP \qquad (2)$$

The quantity C_p is the heat capacity (specific heat) at constant pressure, p is pressure and R is the gas constant. Equations (1) and (2) together with the additional required magnetic relationships can be used to calculate the isothermal entropy changes and the abiabatic temperature changes under corresponding p or B changes. Figure 19 shows the temperature-entropy diagram of constant pressure processes for hydrogen and helium at 1 and 10 atmospheres and corresponding curves for a magnetic material experiencing constant applied fields for fields up to 10 tesla (1 tesla = 10^4 gauss). The ferromagnetic material considered is suitable for use in a very cold magnetic refrigeration system. The Curie temperature of the magnetic material is 40°K (72°R). All of these curves were extracted from Barclay's Ref. 14 and replotted in the format shown which may be more familiar to the reader. The curves for the magnetic material were developed using the molecular field model for the magnetic equation of state and the Debye model for the heat capacity (Refs. 13 and 14) With these models the entropy changes as a function of temperature and magnetic field were found.

It is apparent from Figure 19 that the entropy decreases as the intensity of the applied magnetic field is increased, and that the largest change for an isothermal process occurs at the Curie temperature of 40°K. For an adiabatic process (constant entropy) it is evident that the maximum range of temperature change is about 20°K. Hence, to accommodate larger changes in temperature, the use of different magnetic materials arranged in series in descending Curie temperatures are essential. In gaseous systems, however, larger temperature changes for adiabatic expansion or compression over the pressure ratios shown will take place at higher temperatures.

To realize a magnetic cycle, either the magnetic field can be moved or the ferromagnetic material can be moved (Ref. 9). The various basic methods of moving the magnetic field include: (1) physically moving the magnet that produces the field, (2) moving a shield located between the magnet and the ferromagnetic material, (3) dissipating the magnetic field by resistance heating, and (4) switching the magnetic field to another inductor by means of a special electric circuit. Methods of moving the ferromagnetic material include: (1) reciprocating motion of a piston (constructed of a ferromagnetic material) in and out of a constant field, and (2) continuous rotation of a disk of ferromagnetic material with a portion of the disk passing through the field.

In any of these approaches motion generates irreversible losses. By moving the magnetic field, the field will interact with surrounding conductors and magnetic materials to produce eddy-current and hysteresis losses. Mechanical motion of large magnets produces losses through friction. By moving the magnetic material a constant dc magnetic field can be used, but in a regenerative system the motion of the heat transfer fluid must be in a direction opposite to that of the magnetic material. The minimization of these losses plays a major role in determining the viability of a given approach.

Descriptions of specific systems follow. It may be helpful to keep in mind that whether these systems be mechanical in nature (such as a rotating wheel) or electrical (with a varying applied magnetic field) they all share the common requirement that the ferromagnetic substance must be heated during its

exposure to an applied magnetic field and cooled in the region where it is not exposed to the field (Ref. 15).

a. Solid Ferromagnetic Working-Material Concepts

(1) Stationary Shunt

Kirol and Mills (Ref. 7) have described a simple form of a thermomagnetic generator which consists of a shunt of a solid ferromagnetic material placed in the air gap between the pole pieces of a stationary magnet as shown in Fig. 20. An electrically conducting coil surrounds the shunt and the magnetic flux lines. Some method for cycling the temperature of the shunt material must be provided. In this configuration it is accomplished by cycling hot and cold fluids through passages in the shunt. Changes in the temperature of the shunt material which span its Curie point produce changes in the magnetic flux. This induces voltage in the coil and hence, a current will flow which produces a secondary magnetic field in the coil. By Lenz's law the direction of current flow is such that this secondary field opposes any change in the magnetic flux of the shunt. Thus, during that part of the cycle when the temperature of the shunt is increasing, the secondary field adds to the applied field of the magnet because the shunt field is decreasing. Then, during the time that the temperature of the shunt is decreasing, the secondary field and the applied field are opposed. At each temperature extreme reversal of the secondary field produces a net field change which changes the magnetic entropy thereby allowing heat to be converted to electricity. By continuously cycling shunt temperature, continuous electrical power is produced. However, the lattice specific heat is large compared to the amount of heat that is converted to electricity via magnetic entropy changes; therefore, any practical thermomagnetic generator would have a regenerator which stores sensible heat released during the cooling portion of the cycle and returns it during heating. This use of regeneration greatly enhances the efficiency.

Several analyses of thermomagnetic systems through 1959 predicted efficiencies of less than 1% for nonregenerative cycles; hence, the concept was considered to be impractical. However, in 1984 Kirol and Mills (Ref. 7)

estimated efficiencies as high as 12.8% (75% of Carnot) for a regenerative cycle; consequently, these systems warrant further consideration. Sources of irreversibilities have been identified but their effects on performance have not been evaluated. On the other hand, any system that produces electrical energy at a cost less than the prevailing rates will be economically viable regardless of technical performance values; hence, this is an important factor that should be dealt with early if these systems are to be considered suitable for practical use.

Utilization of the magnetocaloric effect in a thermodynamic cycle for any ferromagnetic material is limited to a temperature range of about 50°C. To effectively use the thermal energy in waste heat streams, however, a converter should be operable over a larger temperature range. A possible method of accomplishing this with a thermomagnetic converter is to stage several units together, each containing a different ferromagnetic material and Curie point. The materials selected must have Curie points that lie in continuous steps covering the range of temperatures needed to recover the waste heat energy. Reference 16 contains a very comprehensive tabulation of many materials, their Curie temperatures, and the references from which the tabulation was obtained. Table 1 (information from Ref. 16) shows some of the compounds, alloys, and their respective Curie temperatures that cover the range of temperatures of waste heat streams.

Performance of thermomagnetic generators can be improved if the applied field is changed by some external means rather than relying solely on the change occurring due to varying permeability of the shunt material. In 1966 Rosensweig (Ref. 15) studied performance of a thermomagnetic generator in which resonance between an inductor and a capacitor was used to vary the applied magnetic field. He predicted that performance increases by a factor of 2 to 10, depending on strength of the applied field. Active control of the magnetic field gives thermodynamic performance equivalent to a rotary recuperative magnetic heat engine if a recuperative cycle is used, and performance equivalent to a reciprocating cycle when a regenerative cycle is used. Rotary and reciprocating generators are discussed in subsequent sections. Several schemes have been identified for efficient switching of a superconducting

magnet to allow active field control (Ref. 9). In very low temperature refrigerators ac losses in the superconductor, although small, result in very significant refrigeration loads (all heat input at 4°K must be removed at about 300°K, with typical coefficient of performance of 0.001 - 0.0015). Use of high temperature superconductors would decrease this parasitic load dramatically.

Reciprocating and regenerative heat engine cycles require that a temperature gradient be established and maintained in the regenerator. In these devices, liquid regenerators are usually used, and conduction and mechanical mixing significantly smear the gradient and hurt performance.

(2) Rotary

Another version of a thermomagnetic generator concept (described in Ref. 10) is shown in the upper part of Fig. 21. It consists of a toroid made of a solid ferromagnetic material which is free to rotate through a magnetic field. The segment of the toroid that is inside the magnetic field at anytime is heated; whereas, that part which is outside the bounds of the field is cooled. Since cooling increases magnetization and heating decreases it (Fig. 18), the cold side of the toroid is attracted into the field region with a larger force than the hot side and hence, a torque is generated which produces a continuous rotation. By suitable arrangement and design a conductor could be placed on the toroid and electricity generated as the conductor crosses the magnetic field. Electrical power could then be extracted from the rotating member by conventional means. This device has the complexity of rotation when compared with the one shown in Fig. 20, but on the other hand does not require cycling hot and cold fluids back and forth to heat and cool the shunt.

The toroid shown in Fig. 21 is porous, however, and contains fluid which is made to flow in the opposite direction of rotation of the toroid. This makes the system regenerative enhancing the efficiency. The important details of how this takes place is not shown. The lower part of Fig. 21 shows the temperature-entropy (T-S) diagram for the cycle as the toroid makes one revolution. The numbers on the toroid correspond to the state numbers on the T-S diagram.

In tracing these processes around the cycle, it is helpful to keep the following in mind: 1) adiabatic magnetization increases the temperature; therefore, constant-temperature magnetization requires heat rejection, and 2) adiabatic demagnetization decreases the temperature; therefore, constant-temperature demagnetization requires heat addition. Beginning at state 1 the working material is hot and is inside the applied magnetic field. As the toroid rotates to point 2, the working material leaves the magnetic field and heat is added (indicated as Q_{in}) from the high-temperature heat source simultaneously in such a way that the process from 1 to 2 is one of isothermal demagnetization. Then as the toroid rotates from point 2 to point 3 there is counterflow heat exchange. The solid working material is cooled by the regenerator fluid that flows from 3 to 2. Between 3 and 4 isothermal magnetization of the toroid occurs as heat is rejected to the low-temperature sink. Then in moving form 4 to 1, the working material is heated by the counterflowing regenerator fluid. The heat that was removed during the cooling process (2 to 3) is now returned to the working material. Thus, the cycle has been completed and the area inside the T-S diagram represents the amount of heat converted to work. The entropy of the high-field process is smaller than the entropy of the low-field process.

This cycle is an Ericsson cycle; however, magnetic devices can also be made to operate on other cycles. For example, the isothermal processes 1 to 2 and 2 to 4 can be made adiabatic which would convert the T-S diagram of Fig. 21 into a Brayton cycle.

(3) Reciprocating

Reciprocating heat engines are similar to reciprocating heat pumps. A discussion of reciprocating engines appears in Ref 10. as follows: They consist of a core of magnetic working material inside a vertical column of regeneration fluid (Fig. 22). The core moves in and out of the bore of a superconducting solenoid magnet as the regenerator moves vertically relative to the core, to add and remove heat. Work output results from the fact that cold core material is more magnetic than warmer material, and more work is released as the cold core enters the field, than is required to move the core when it is

hot. Studies of magnetic heat pumps have indicated that rotary machines have better performance than reciprocating machines; consequently, most of the work has been focused on rotary devices.

A reciprocating heat pump is thermodynamically equivalent to an Active Magnetic Regenerator (described in the next section) in which the field is actively switched on and off. When motion of the magnetic core is used to achieve the field change, heat is converted to mechanical work. When field switching is used, heat is converted directly to electrical power. For heat pumps and heat engines, regardless of whether field switching or core motion is involved, an active core with a single Curie temperature working material and a second thermodynamic medium for regeneration results in performance significantly below that of a rotary (recuperative) heat pump or heat engine. For both cases, a core with graded Curie temperature material in which the active magnetic material also serves as regenerator may provide improved performance.

(4) Active Magnetic Regenerative Thermomagnetic Generators (AMRTG's)

The overall efficiency of a system may be increased by connecting a number of generators in series, that is, ferromagnetic materials which have descending Curie temperatures. In such a series arrangement the heating fluid leaving the first stage enters the second, then the third, and so on. A similar arrangement can be used for the cooling fluid (Ref. 15). The AMRTG system consists of such a series arrangement. It contains several porous ferromagnetic materials of different Curie temperatures, arranged in such a way that by cycling the materials thermodynamically, thermal energy over larger temperature ranges can be converted to electricity than is possible with a single Curie-point system. This concept can be configured in either a reciprocating mode or a wheel mode. For the purpose of this discussion the wheel mode is considered. The different materials are staged, being arranged in gradually decreasing Curie temperature as annular segments of the wheel. A sketch of this concept is shown in Fig. 23. This system operates as a single unit without the need of any interstage heat exchangers between each of the

segments. A similar wheel-type system but operated as a refrigerator has been investigated by Barclay and is described in Refs. 12, 13 and 14.

It should be noted that the sketch of the system in Fig. 23 is simply intended to convey the idea of the concept. It is not intended to infer that the regenerators be sized or located precisely as shown, nor that the applied magnetic field be tailored precisely as indicated. It is apparent from Fig. 23 that the AMRTG system in this configuration closely resembles the single Curie-point rotary system shown in Fig. 21. The operation is similar in that the cold magnetized portion of the wheel at the bottom is attracted by the applied magnetic field with greater force than the demagnetized warmer part of the wheel at the top. Hence, a torque is generated and the wheel rotates as indicated. Because of the composite structure of the wheel, tailoring of the applied magnetic field distribution in accordance with the requirements of the magnetic materials may be beneficial.

In the magnetic field region the ferromagnetic materials are heated by hot fluid which is forced through the porous segments through one, then the next, and so on in the stationary heat-addition regenerator. This fluid in turn becomes cooled by the colder porous bed. The fluid that leaves the bed is then cooled an additional amount in an external heat exchanger (not shown) and from there is forced through the porous segments in the heat-rejection regenerator. This cools the porous elements and magnetizes them. Simultaneously the fluid is heated by the warmer bed. Additional external heating of the fluid is then needed before the cycle is repeated. The process is referred to as active magnetic regeneration because a portion of the cyclic reheating and recooling of the heat transfer fluid is brought about by the ferromagnetic material segments themselves. The efficiency of such a system is very sensitive to the performance of the regenerator.

The rotary configuration of the AMRTG with its regenerator segments may be classified as a rotary regenerator heat exchanger; even though in this case the same fluid continuously passes through the system alternating between being cooled by the rotor and being heated by another segment of the rotor.

A narrative and graphic description of the thermal wave front that passes through the porous bed as it is being alternately heated and then cooled by the penetrating fluid is described by Barclay in Refs. 12 and 14. A mathematical formulation of this process for the refrigerator consisting of a one-dimensional system appears in Ref. 14. Numerical methods are required to obtain solutions to the complex partial differential equations which are both time and space dependent. No solutions in terms of results are shown in Ref. 14; however, results for particular simplified systems consisting of both magnetic and non-magnetic porous materials of stationary beds are given in terms of temperature profiles versus distance. It is also pointed out that the rates of magnetization and demagnetization are limited by the heat transfer, which for a rotating system would place a limit on the wheel speed. In practice this is estimated to be less than 1 Hz. If the heat transfer ratio could be improved substantially, the next limitation is believed to be the eddy current power which would probably become significant at between 5 to 10 Hz. If both of these limitations were eliminated, the upper limit on cycle frequency is given by the spin-lattice relaxation rate, which for certain materials such as gadolinium compounds (used for refrigeration) would be about 1 kHz.

Regenerator performance optimization for various porous regenerator geometries has been explored by Barclay and Sarangi (Ref. 17). Discussions of temperature-entropy diagrams for a variety of ideal and non-ideal thermodynamic processes and cycles are given in Ref. 18, and a general review of magnetic refrigeration appears in Ref. 19.

An active magnetic regenerative refrigerator for operation below 20°K has been built and tested at MIT (Ref. 20). It achieved an efficiency of about 7% of Carnot, which is quite good compared to other technologies at that temperature and compared to magnetic refrigeration experience to date.

Since the focus of the work done so far has been on refrigeration, the analyses should be extended to direct thermal-to-electric conversion systems. The heat transfer processes should also be reviewed to determine whether modifications can be incorporated to increase the heat transfer rates in the

porous beds. Then, if the performance of such a system seems promising from an analytical standpoint, laboratory verification experiments should be initiated.

(5) Combined Thermomagnetic and Pyroelectric System.

Another system, which consists of a combination of the thermomagnetic concept and a pyroelectric device (Ref. 1) but which is only in the suggestion stage, should also be explored. It seems possible that these two concepts might be beneficially coupled with resonance between the inductor and capacitor thereby transferring energy between a magnetic field and an electric field.

b. Ferrohydrodynamic Working-Fluid Concepts

The discussions on thermomagnetic energy converters so far have focused on working substances that are solid ferromagnetic materials. It has also been shown, however, that very fine particles, less than 100 angstroms in size of ferromagnetic materials can be suspended in carrier liquids which then experience an appreciable body force in the presence of a non-uniform magnetic field (Refs. 21 and 22). Carrier liquids can be, for example, either a hydrocarbon, a diester, water, a liquid metal, or some other liquid. The number of particles per unit volume in such a colloidal suspension can be very large, characteristically between 10^{15} and 10^{19} particles per cubic centimeter (Ref. 22). These ferrohydrodynamic fluids are stable, strongly polarizeable, and furthermore, the body force is temperature dependent.

A schematic diagram of a simple thermomagnetic converter that uses a liquid ferrohydrodynamic material (ferrofluid) as the working substance, is shown in Fig. 24. Here, the circulating ferrofluid essentially replaces the torroidal ring of Fig. 21. As shown in Fig. 24, the fluid is cooled and thereby magnetized as it flows through a counterflow heat exchanger. It then passes through a magnetohydrodynamic generator where the energy is converted to electrical power. Then, as the ferrofluid enters the heater, it is still cold and highly magnetized. Hence, the magnetic field generated by the solenoid draws the ferrofluid into the solenoid region where the ferrofluid is heated above its Curie temperature and thereby demagnetized. As a consequence, the

force that draws the ferrofluid into the solenoid region on the cold side is greater than that which acts to prevent it from moving out on the hot side. Hence, the combination of the heat exchanger and the solenoid acts as a pump and an increase in pressure results together with the induced motion. This increase in pressure combined with the fluid motion can then be converted directly into electricity in the magnetohydrodynamic generator, since the ferrofluid is an electrical conductor.

As the ferrofluid flows through the combined solenoid-heater segment of the generator, shown in Fig. 24, work is done on the fluid as a consequence of the interaction of the solenoid-applied magnetic field with the ferromagnetic particles dispersed in the fluid. In addition to the work, heat is added to the fluid simultaneously. The behavior of the fluid imposed by these effects is treated macroscopically and the dispersion is handled as a continuum. This is the approach that has been used by researchers to analyze the system.

Several analyses of reversible thermodynamic cycles of ferrofluids appear, for example, in Refs. 22, 23 and 24. Expressions for efficiency and power per unit mass have been developed. Maximum efficiency appears to be about 75% of Carnot for a single stage system. Also, losses in a particular system have been estimated.

The stability of ferrofluids, which consist of a liquid metal carrier containing particles of iron or iron-nickel alloys, was investigated by the authors of Ref. 25. Stability refers to the time duration in which the characteristics and properties of the ferrofluid are not significantly altered. It is shown that if the particles are comparatively too large, or become too large by clustering or by diffusional growth, the fluids tend to become unstable. It was concluded that to produce a stable ferromagnetic liquid requires: (1) a distribution of particles of diameter less than 30 angstroms in the case of iron, (2) the particles to be coated with tin to prevent diffusional growth, and (3) preferably some additional repulsion between particles to prevent aggregation. The preparation of a fluid which would be stable for many months does seem to be a real possibility.

Low magnetic density of ferrofluidic materials increases the ratio of sensible heat to magnetic specific heat of the working material. In solid working material cycles the recuperative heat load (commonly called recirculating heat) is about 20 times as large as the heat flow into the cycle, and recuperation is the major source of irreversibility. The recirculating heat ratio is even larger with ferrofluidic working material, increasing the difficulty of achieving good efficiency. It is imperative that magnetization of the working fluid be increased to the maximum extent possible without destroying stability of the fluid.

c. Technical Research Needs of Thermomagnetic Concepts

Reported performance on the ferrohydrodynamic concepts is based mainly on ideal steady-flow thermodynamic cycle analyses. Hence, most of the more realistic flow and energy exchange processes, which include loss mechanisms, have not been taken into account. Analytical work that needs to be done includes the fluid mechanics, heat transfer and thermodynamics of an electrically conducting fluid as it flows through the magnetic field gradient regions of the solenoid heater and through the electric generator. Loss mechanisms should be taken into account. An analysis should also be done to determine performance of systems staged in series in which ferromagnetic materials with different Curie points are selected so that larger heat-source and heat-rejection temperatures can be accommodated than is possible with a single-stage single Curie-point unit. Experiments should then be conducted with systems that are the most promising.

Most of the tabulated Curie points of ferromagnetic materials are based on calculations. The Curie points should be verified experimentally for those materials selected to establish performance. Optimization of material properties may also require development of new alloys.

For solid working material generators more refined performance predictions are needed which take into account sources of irreversibilities including regenerative heat transfer across a non-zero temperature difference. In addition, performance of working substances that have intermediate Curie

temperatures (100°F to 1300°F) should be analyzed. Also, thorough definitions of desireable properties of the working material should be accomplished and real materials with these properties should be identified. Then, performance verification and regenerative heat transfer evaluation should be done experimentally. Material development and property determination should also be done experimentally.

Active Magnetic Regenerative Thermomagnetic Generators with both active and passive control of the applied field should be investigated. As a first step, the analyses which have been made by Barclay, et al (Refs. 14 and 18) for refrigerators should be reviewed and extended to direct thermal-to-electric conversion systems. Then, if the performance of such a system seems promising from an analytical standpoint, laboratory verification experiments should be initiated.

Since no known analysis of the combined thermomagnetic-pyroelectric system exists, this combination should be analyzed after more work has been done on the AMRTG system.

2. Thermoelastic Converters (Nitinol Engine)

A variety of thermoelastic converter system concepts have evolved which are based on the use of metal alloys that possess a unique mechanical shape "memory" property. These concepts are referred to as Nitinol heat engines and they transform heat into mechanical shaft work and then can transform the mechanical work into electricity by conventional means. Consequently, they are not true direct conversion systems. A discussion of them is included here because their operation is feasible at hot water temperatures and over small temperature differences which make them suitable for converting the thermal energy in industrial waste heat streams to electrical energy. In addition, the working medium is a solid metal which puts them in a novel innovative category, and they also appear to be comparatively simple. Seals and heat exchangers are not required. For one of the engine configurations conceived, continuous engine operation is initiated and maintained by simply immersing the appropriate segment of the belt (which is the working medium that drives a

power pulley) into hot water and another segment of the same belt into cold water. Descriptions of the characteristic behavior of the working material that makes this possible, and descriptions of engine configurations are given in the following paragraphs.

The solid-state working medium of the thermoelastic converter is Nitinol which is a generic name for a range of alloys of nickel and titanium discovered at the Naval Ordnance Laboratory in the 1960's. The name Nitinol is derived from Nickel, Titanium, Naval Ordnance Laboratory. Nitinol undergoes an energetic solid-solid phase transformation when heated to a critical transition temperature. The transition corresponds to a transformation from a martensitic (orthorhombic) phase to a parent austenitic (cubic) phase. It is this transformation that results in the thermoelastic and mechanical shape "memory" effects. A specimen of Nitinol may be superelastically deformed about 5 percent at a low temperature (below the transition temperature) by applying a load at moderately low stress. Then, if the temperature of the specimen is raised above the transition point, the specimen will recover ("snap back" to) its earlier shape, which is the shape "memory" effect. The forces generated by the specimen during the hot recovery process can greatly exceed those required during the cold deformation process and may be as much as 200 times greater than those exerted by bimetals (Ref. 26). Therefore, the specimen has the ability to perform mechanical work from heat input. Furthermore, the transformation temperature of the Nitinol family of alloys can be manipulated over a remarkably wide range, from about -273°C to 100°C (-459°F to 212°F) by altering the nickel-titanium ratio and by adding small amounts of other elements (Ref. 26).

A large variety of useful applications have been found for the "memory" metals. A few of these include switches, circuit breakers, hydraulic fluid-line couplings, electrical connectors that form high compression fits yet can be quickly released and recoupled, and various biomedical devices for artificial limb joints, orthopedic bone fractures, etc. (Refs. 26 and 27). Even a braille device that will allow blind people to use a word processor is under development (Ref. 28). Several companies have been established that specialize in the manufacture of such devices. The focus here, however, is on

the potential application of Nitinol as the working medium in a heat engine that can convert low-grade energy such as waste heat in industrial streams to electrical energy.

Nitinol heat engines have two fundamental advantages over other conversion systems. First, the solid-state working medium provides superior heat transfer characteristics when compared to gaseous systems. This eliminates the need for separate heat exchangers. Secondly, Nitinol is corrosion-resistant and need not be isolated from an environment such as hot water. This eliminates the usual requirement for seals. These factors result in mechanically simple heat engines.

An illustration of the mechanical shape "memory" effect which is the basis of Nitinol engine operation (Ref. 29) is shown in Fig. 25. Sketch (A) shows an undeformed specimen at a cold temperature T_1, which is less than the transition temperature. A weight, W_1 pulls the specimen down, as shown in (B), to a deformation distance d_1. The total weight attached to the specimen is increased by the addition of another weight W_2, as shown in (C). Then as indicated in (D), when the specimen is heated to above the transition temperature, it recovers its original shape lifting both weights in the process. The net work performed during these operations is given by the force-distance product W_2d_1.

In a thermodynamic sense it may, at first, seem incredible that there can be repeated net work output during such cyclic phase changes of the Nitinol. However, by considering an analogous phase change cycle in which a given amount of water is converted to steam and the same steam back to water, with which the reader may be more familiar, the fact that there is net work output may become more apparent. For example, at atmospheric pressure, a strictly change of phase process from water to steam at the saturation temperature requires the same amount of thermal energy (latent heat) added as is released when the process is reversed. If, however, the pressure is raised during heating, but kept lower during cooling, the latent heats will differ and there will also be sensible heat involved with associated temperature changes. So it is with the Nitinol when the weight, W_2 is added; the cycle involves more than just phase

changes, and hence, the net work results from the heat that is added to raise the additional weight.

Numerous engine configurations have been conceived, constructed, and operated in a laboratory environment (Refs. 30 and 31). Examples are various types of offset crank engines which operate in a manner similar to hot gas reciprocating engines but with the thermodynamic working material being Nitinol instead of a gas. Sketches of these are not shown here but do appear in Ref. 31. Brief descriptions of some follow.

The first well publicized Nitinol heat engine was an offset crank engine built by Banks in 1973 (Ref. 32). At a temperature differential of 23°C between the hot and cold water which provided the heating and cooling of the Nitinol, an engine speed of 69 rpm was attained with a power output of about 0.23 Watt. The engine completed more than 100 million cycles of operation without evidence of fatigue or degradation failure.

Another configuration of an offset crank engine was built at McDonnell Douglas in 1974 (Ref. 31). Water was used as the heat source and air as the cooling medium. In this arrangement six helixes of Nitinol wire, shaped like coiled springs were connected between the peripheries of a small rotating central hub and a large rotating outer wheel. The hub axle was offset from the wheel axle by a fixed crank. A temperature differential of about 3°C was sufficient to initiate engine operation. Because of the relatively slow heat transfer between the Nitinol helixes and air, both the engine speed and output power were low.

Still another variation of the offset crank type was patented by Hochstein in 1977 (Refs. 31 and 33). Nitinol elements in the form of flat strips were connected between a rotating central hub and cams that ride on a sinusoidally curved rim. The strips were strained (bent) by the engine in the cold quadrant, and did work during the straightening in the hot quadrant. Engines of this type including regeneration are reported to have delivered 10 to 20 Watts of power at maximum speeds of 70 rpm.

A design that bears a striking resemblance to an internal combustion engine was patented by Smith in 1978 (Refs. 31 and 34). This configuration uses Nitinol in the form of helical coils within closed cylinders through which hot and cold fluids (air/water) are circulated alternately. One end of each coil is connected to the bottom of a cylinder and the other end to a conventional crankshaft. Presumably a number of such coils and cylinders could be arranged similar to those of a piston engine.

The offset crank engines that have been reported have been comparatively easy to construct and have almost always worked the first time, but they have a number of limitations that must be overcome before being seriously considered for commercial development. Among these limitations are: low power densities and low cycle speeds, large engine volumes, inefficient and awkward cooling systems, alternating replacement of hot and cold reservoirs, metal-to-gas heat transfer and nonuniform heating and cooling of Nitinol elements.

The most successful more recent designs are referred to as thermoturbine engines. In the turbine configurations a continuous loop of Nitinol wire or a helix is guided by idlers through cold and hot water baths and over differential pulleys as shown in Fig. 26. One of the pulleys serves as an expander (or turbine) and extracts power from the moving loop. The loop of Nitinol wire moves around the pulleys and idlers because tension in the loop on the hot side is greater than tension on the cold side. The expander pulley is connected mechanically to a compressor (or pump pulley) that does work on the loop. The work performed by the loop of wire on the expander exceeds the work performed on the loop by the compressor, which results in net work output. A number of engine variations were conceived and constructed using Nitinol helixes or wire, different methods of coupling the expander and compressor pulleys, and variations in heat source/sink configurations. An engine design of this type including regeneration was patented by Johnson in 1977 (Refs. 35 and 36).

The configuration shown in Fig. 26 was built by Cory (Ref. 31). It consisted of a close-wound Nitinol wire helix (3 mm O.D.) for the belt, with the expander-compressor pulleys of the same diameter but geared together to run

at different speeds. The engine, when operated between 5°C and 70°C, attained a speed of 2500 rpm and produced about 0.5 Watt of power.

In DOE sponsored work, McDonnell Douglas built and tested a 35 Watt Nitinol heat engine module (Ref. 37). Measurements were obtained of the shaft power output vs. rpm, and also of the power delivered by the Nitinol, that is, the Nitinol-delivered torque times the angular frequency of the shaft. The maximum shaft power output was reported to have been about 32.5 watts at an engine speed of about 235 rpm. At these conditions the hot and cold water temperatures were about 75°C and 10°C (165°F and 49°F) respectively. The number of Nitinol helixes in the combined parallel-series engine was 81. Design of the maximum helical pitch was consistent with a 10^5 cycle lifetime based on strain-lifetime correlations.

Power delivered by the Nitinol exceeded the shaft output power. The lower values of the shaft power resulted from frictional losses, such as bearings, and from parasitic losses, such as water carried out of the troughs by the helical Nitinol bands. The speed and torque of the output shaft were measured by a dynamometer which consisted of three components: a tachometer, a frequency-to-voltage converter and controller, and a hysteresis brake. The Nitinol-delivered power was obtained from load-cell force measurements, the radius of the power roller, and the measured angular frequency of the shaft. In addition, under stall conditions an upper limit of shaft output power was determined from the torque at stall times shaft frequency. Hence, this was an increasing linear relationship vs. shaft rpm. The stall value at maximum shaft output power speed substantially exceeded the measured output and represents the power which would be produced if there were no power losses and no water carryover or mixing.

Considerable effort was also devoted to Nitinol helix conditioning. During initial thermal/mechanical cycling of a freshly annealed Nitinol helix, the force-length-temperature characteristics change significantly. However, the rate of change of these characteristics decreases with the number of cumulative cycles and eventually the properties become essentially stable for

the lifetime of the element. After becoming stabilized the helix can then be used on a constant-length engine.

After this experimental program was completed at McDonnell Douglas Astronautics Company, the company phased out these energy related activities and no further experimental work on Nitinol heat engines has been done there.

In Japan, during 1981 and 1982, the Ministry of International Trade and Industry (MITI) sponsored the development of a 500 Watt Nitinol heat engine (Ref. 38). The engine was constructed as an assembly of three modules of exactly the same structure. The pulleys and idlers were connected by a total of 252 Nitinol helixes arranged in parallel which actually produced a maximum output of 665 Watts at 201 rpm. The present status of the Japanese engine is not known. However, it is possible that the developmental activity was halted because of projected high cost.

The efficiency of most Nitinol heat engines is generally low (1-3%), partly because they are nonregenerative and also because they operate over small temperature differences. Higher efficiency is obtainable by employing regenerative heat flow. In one regenerative Nitinol heat engine, the efficiency was measured at 6.5% for operation between 5°C and 80°C (Ref. 39). The Carnot efficiency for this range is 21%. Thus, the demonstrated fraction of Carnot was 0.31. According to Ref. 39, calculations indicate that between 70 and 80% of Carnot should be feasible with new heat engine designs. In the near term, this means that efficiencies as high as 17% over this temperature range are possible with Nitinol as the working material. All of these numbers are for conversion of heat to mechanical work. Additional losses are incurred by conversion of the mechanical work to electricity. Perhaps the use of Nitinol would be more promising as a direct thermal-to-electric conversion device if some means of accomplishing this were conceived. The specific work that Nitinol will produce with present designs is about 400 J/kg (Ref. 40). At 1 to 10 Hz, this gives 400 to 4000 Watt/kg electrical power output.

If efficiencies of 70 to 80% of Carnot were achievable, thermoelastic converters might appear attractive, but there are other technical problems

also. These heat engines have been plagued with variations in mechanical properties of the Nitinol, which generally results in mechanical failure. Both the DOE and the MITI engines have encountered material properties variability. Variations in the thermoelastic properties of the helixes can substantially degrade the performance of the heat engine. It has been found that the mechanical properties (e.g., the stress-strain curve) of thermoelastic materials are very dependant on the history of the mechanical and thermal processing.

A characteristic behavior of Nitinol has been that it does not consistently return exactly to its original undeformed and thermal states after having undergone elastic deformation. The three mechanical behavior variables: force, length and temperature, are not adequate to define the state of the material. This led to the belief by some researchers that the purity and composition of the alloy was not being controlled with sufficient accuracy in the manufacturing process to eliminate this behavior. Hence, one main focus of Nitinol development was on the metallurgical aspects of the material (Ref. 27).

Other researchers, namely, J.S. Cory (Ref. 41), performed numerous experiments with Nitinol, worked on correlations of data and on the normalization of material properties to determine whether this behavior could be consistently accounted for in some other way. As a consequence of these experiments and analyses, Cory concluded that the observed behavior in most instances could be accounted for by hysteresis effects. This led to the development of macroscopic nonequilibrium thermodynamics for application to hysteresis phenomena of Nitinol (Refs. 42 and 43). In this approach it was established that 7 variables instead of 3 were needed to define thermodynamic paths and state points. These include the 3 mechanical behavior variables stated previously, the transition temperature associated with the change in material structure, and 3 additional mechanical "history" variables of force, length, and temperature. It was concluded that a minimum of measured state equation coefficients and measured heat capacities, or estimated data, could be used to describe quantitatively the complex mechanical and thermal behavior on the paths in the shape-memory region.

A second issue which needs to be addressed to advance the technology base for thermoelastic conversion centers on device design. Existing designs extract only about 1 Watt per helix of Nitinol. This is not bad when compared with, for example, thermoelectrics (which require very many parts to produce 1 Watt). However, the associated pulleys and bearings add significantly to the cost and complexity of the device. New designs are needed in which the number of parts is reduced so that Nitinol devices can approach their potential for low cost, low temperature conversion.

Reference 40 contains the development of a model for estimating costs for low-grade thermal energy conversion utilizing Nitinol power plants. This is a first-cut analysis in which the Nitinol heat engine portion of the power plant is separated from those portions of the plant for which cost estimates can be made using conventional procedures. It was estimated that the heat engine capital cost per unit power capacity was about 15¢ per Watt, and the costs of produced energy for the Nitinol heat engine portion of the plant, including the cost of capital and the operation, maintenance, and replacement costs, were estimated to be approximately 0.74¢/KW-hr. The principal conclusion of this study was that Nitinol power plants for low-grade thermal energy conversion may have significant cost advantages over conventional fossil fuel power plants. **It was also pointed out that any conversion system which produces energy at a cost less than the prevailing rates will be economically viable, independent of efficiency, or any other purely technical criterion.**

It appears that the next phase of Nitinol heat engine development should consist of design, construction and testing of a multikilowatt prototype for a particular application such as conversion of thermal-to-mechanical energy from waste heat streams or from geothermal sources. Thus, the status of Nitinol heat engine development has already passed through the phase that would normally be supported by ECUT unless a new system concept were to evolve for converting thermal-to-electrical energy directly.

ACKNOWLEDGEMENTS

Discussions on thermomagnetic systems with Dr. John Barclay, Manager of the Thermomagnetic Device Department at the Astronautics Corporation of America, and with Mr. Geoffrey Green, Section Leader of the Cryogenics Group at the David Taylor Research Center were very helpful and are greatly appreciated.

The section on thermoelastic converters was developed from the referenced documents and from personal communications with various people who are knowledgeable of the behavior of Nitinol, and with those who have also engaged in the development of Nitinol heat engines. A special thank you is extended to Dr. J.S. Cory, President of Cory Laboratories, who also reviewed the writeup. Discussions with the following individuals, in particular, are also greatly appreciated: Dr. A.D. Johnson, President of TiNi Alloy Co.; Dr. L.M. Schetky, Chief Scientist of Memory Metals, Inc.; Dr. D. Hodgson, President of Shape Memory Applications; Dr. J.L. McNichols, Principal Scientist at McDonnell Douglas Astronautics Co.; Mr. E.C. Cady, Manager of Advanced Propulsion at McDonnell Douglas Astronautics Co.; Dr. R.B. Olsen, Chief Scientist of Chronos Research Laboratories; Dr. J. Holthuis, Technical Scientific Coordinator at the Lawrence Berkeley Laboratory; and Mr. R.M. Banks, President/Owner of R.M. Banks and Associates.

REFERENCES

1. P.F. Massier, "ECUT Direct Conversion Technology Project Annual Report CY 1986", JPL D-3707, Jet Propulsion Laboratory, Pasadena, California, January 15, 1987.

2. P.F. Massier, "ECUT Direct Conversion Technology Annual Summary Report CY 1987", JPL D-4856, Jet Propulsion Laboratory, Pasadena, California, January 7, 1988.

3. R.B. Olsen, Private Communication, February, 1988.

4. D.D. Huxtable and M. Olszewski, "Industrial Waste Heat Utilization for District Heating", Proceedings of the 15th Intersociety Energy Conversion Engineering Conference, pp. 910-914, 1980.

5. M.L. Underwood, R.M. Williams, B. Jeffries-Nakamura, C.P. Bankston and T. Cole, "Progress in AMTEC Electrode Experiments and Modeling", Proceedings of the 23rd Intersociety Energy Conversion Engineering Conference, Vol. 1, pp. 227-233, July 31 - August 5, 1988.

6. R.M. Williams, M.E. Loveland, B. Jeffries-Nakamura, M.L. Underwood, C.P. Bankston, H. LeDuc, and J.T. Kummer, "Kinetics and Transport at AMTEC Electrodes," in preparation.

7. L.D. Kirol and J.I. Mills, "Numerical Analysis of Thermomagnetic Generators," Journal of Applied Physics, Vol. 56, No. 3, pp 824-828, August 1, 1984.

8. R.M. Bozorth, Ferromagnetism, D. Van Nostrand Co., Inc., Princeton, New Jersey, Sixth Printing, 1961.

9. J.R. Hull and K.L. Uherka, "Magnetic Heat Pumps", Proceedings of the 23rd Intersociety Energy Conversion Engineering Conference, Vol. 2, pp. 531-536, July 31 - August 5, 1988.

10. L.D. Kirol, "Magnetic Heat Engine Preliminary Study," Idaho National Engineering Laboratory Report, No. EGG-SE-6718, November, 1984.

11. W.P. Pratt, Jr., S.S. Rosenblum, W.A. Steyert, and J.A. Barclay, "A Continuous Demagnetization Refrigerator Operating Near 2K and a Study of Magnetic Refrigerants," Cryogenics, pp 689-693, December 1977.

12. J.A. Barclay, "An Analysis of Liquifaction of Helium Using Magnetic Refrigerators," Los Alamos National Laboratory Report LA-8991, UC-38, December 1981.

13. J.A. Barclay, "Magnetic Refrigeration for Spacecraft Systems", ASME Paper No. 81-ENAS-47, presented at the Intersociety Conference on Environmental Systems, San Francisco, California, July 13-15, 1981.

14. J.A. Barclay, "Theory of an Active Magnetic Regenerative Refrigerator", Los Alamos report LA-UR--83--1251, 1982.

15. R.E. Rosensweig, "Theory of an Improved Thermomagnetic Generator", Proceedings of the IEE, Vol. 114, No. e, pp. 405-409, March 1967.

16. T.F. Connolly and E.D. Copenhaver (compilers), Bibliography of Magnetic Materials and Tabulation of Magnetic Transition Temperatures, Solid State Physics Literature Guides, Vol. 5, IFI/PLENUM, New York, Washington, London, 1972.

17. J.A. Barclay and S. Sarangi, "Selection of Regenerator Geometry for Magnetic Refrigerator Applications", presented at the ASME Annual Winter Meeting, New Orleans, Louisiana, December, 1984, Cryogenic Processes and Equipment, p. 51, 1984.

18. C.R. Cross, J.A. Barclay, A.J. De Gregoria, J.R. Jaeger and J.W. Johnson, "Optimal Temperature-Entropy Curves for Magnetic Refrigeration", presented at the Cryogenic Engineering Conference, St. Charles, Illinois, June 1987.

19. J.A. Barclay, "Magnetic Refrigeration: a Review of a Developing Technology", presented at the Cryogenic Engineering Conference, St. Charles, Illnois, June 1987.

20. C.P. Tausczik, "Magnetically Active Regeneration", Massachusetts Institute of Technology, PhD Thesis, October 1986.

21. E.L. Resler and R.E. Rosensweig, "Magnetocaloric Power," AIAA Journal, Vol. 2, No. 8, pp 1418-1422, August, 1964.

22. R.E. Rosensweig, J.W. Nestor, and R.S. Timmins, "Ferrohydrodynamic Fluids for Direct Conversion of Heat Energy," AICHE, Industrial Chemical Engineering Symposium Series, No. 5, pp 104-118, 1965.

23. J.L. Neuringer and R.E. Rosensweig, "Ferrohydrodynamics," The Physics of Fluids, Vol. 7, No. 12, pp 1927-1937, December, 1964.

24. L. Brillouin and H.P. Iskenderian, "Thermomagnetic Generator," Electrical Communication, Vol. 25, pp 300-311, 1948.

25. J. Popplewell, S.W. Charles and R. Chantrell, "The Long Term Stability of Magnetic Liquids for Energy Conversion Devices," Energy Conversion, Vol. 16, pp 133-138, Pergamon Press, 1977.

26. L.M. Schetky, "Shape Memory Alloys," Scientific American, Vol. 241, No. 5, pp. 74-82, November 1979.

27. C.M. Jackson, H.J. Wagner, and R.J. Wasilewski, "55-Nitinol---The Alloy With A Memory: Its Physical Metallurgy, Properties and Applications," NASA-SP 5110, 1972.

28. L.M. Schetky, Private Communication, March 1988.

29. W.J. Buehler, and D.M. Goldstein, "Conversion of Heat Energy to Mechanical Energy," U.S. Patent 3,403,238, September 1968.

30. D.M. Goldstein and L.J. McNamara, Editors, Proceedings of the Nitinol Heat Engine Conference, sponsored by U.S. Department of Energy and U.S. Naval Surface Weapons Center, Silver Spring, Maryland, September 26-27, 1978.

31. W.S. Ginell, J.L. McNichols, Jr., and J.S. Cory, "Nitinol Heat Engines for Low-Grade Thermal Energy Conversion", Mechanical Engineering, Vol. 101, No. 5, pp. 28-33, May 1979.

32. R. Banks. "The Engine That Runs on Sunshine", Popular Science, pp 87-146, April 1974; "Energy Conversion System", U.S. Patent 3,913,326, (1975).

33. P.A. Hochstein, "Thermal Energy Converting Assembly", U.S. Patent 4,037,411, July 1977.

34. W.K. Smith, "Compressed Memory Engine", U.S. Patent 4,086,769, May, 1978.

35. A.D. Johnson, "Memory Alloy Heat Engine and Method of Operation", U.S. Patent 4,055,955, November, 1977.

36. A.D. Johnson, "Nitinol Heat Engines", Proceedings of the 10th Intersociety Energy Conversion Engineering Conference, pp 530-534, 1975.

37. J.L. McNichols, P.C. Brookes, W.S. Ginell, and J.S. Cory, "Final Report, Prototype Nitinol Heat Engine", McDonnell Douglas Astronautics Co., MDC G9290, April 1981.

38. H. Tanaka, M. Konda, and T. Okuda, "A Study of the High-Power Nitinol Heat Engine", Proceedings of the 20th Intersociety Energy Conversion Engineering Conference, p. 2.729-2.734, 1985.

39. A.D. Johnson, "Experimental Results on a Continuous-Band Nitinol Heat Engine", Proceedings of the Nitinol Heat Engine Conference, sponsored by U.S. Department of Energy and U.S. Naval Surface Weapons Center, Silver Spring, Maryland, pp 8-1 to 8-13, September 26-27, 1978.

40. J.L. McNichols, J.S. Cory, and E.H. Curtis, "Approach to Nitinol Power Plant Cost Analysis", Journal of Energy, Vol. 6, No. 6, pp 399-405, November 1982.

41. J.S. Cory, Private Communication, February, 1988.

42. J.S. Cory and J.L. McNichols, Jr., "Nonequilibrium Thermostatics", Journal of Applied Physics, Vol. 58, No. 9, pp. 3282-3294, November 1, 1985.

43. J.L. McNichols, Jr. and J.S. Cory, "Thermodynamics of Nitinol", Journal of Applied Physics, Vol, 61, No. 3, pp. 972-984, February 1, 1987.

Table 1. Ferromagnetic Compounds/Alloys and Their Curie Temperatures

COMPOUND/ALLOY	CURIE TEMPERATURE, °K
Fe	1043 (1418 °F)
Fe - Ni: 55% Fe	956
Fe Al	923
Fe_3 Cr	893
Fe_3 O_4	858
Fe_8 Co_{12} Al_3 B_6	815
$Fe_{0.75}$ $Ga_{0.25}$	760
Fe Pt	743
Fe_3 P	686
Fe_5 B_2 P	628
Fe B	598
Fe_3 B O_6	508
Fe_5 Ge_3	485
Fe_3 C	483
Fe_2 Mn Ge	433
Fe_5 Si_3	381
Fe_3 Se_4	318 (113 °F)

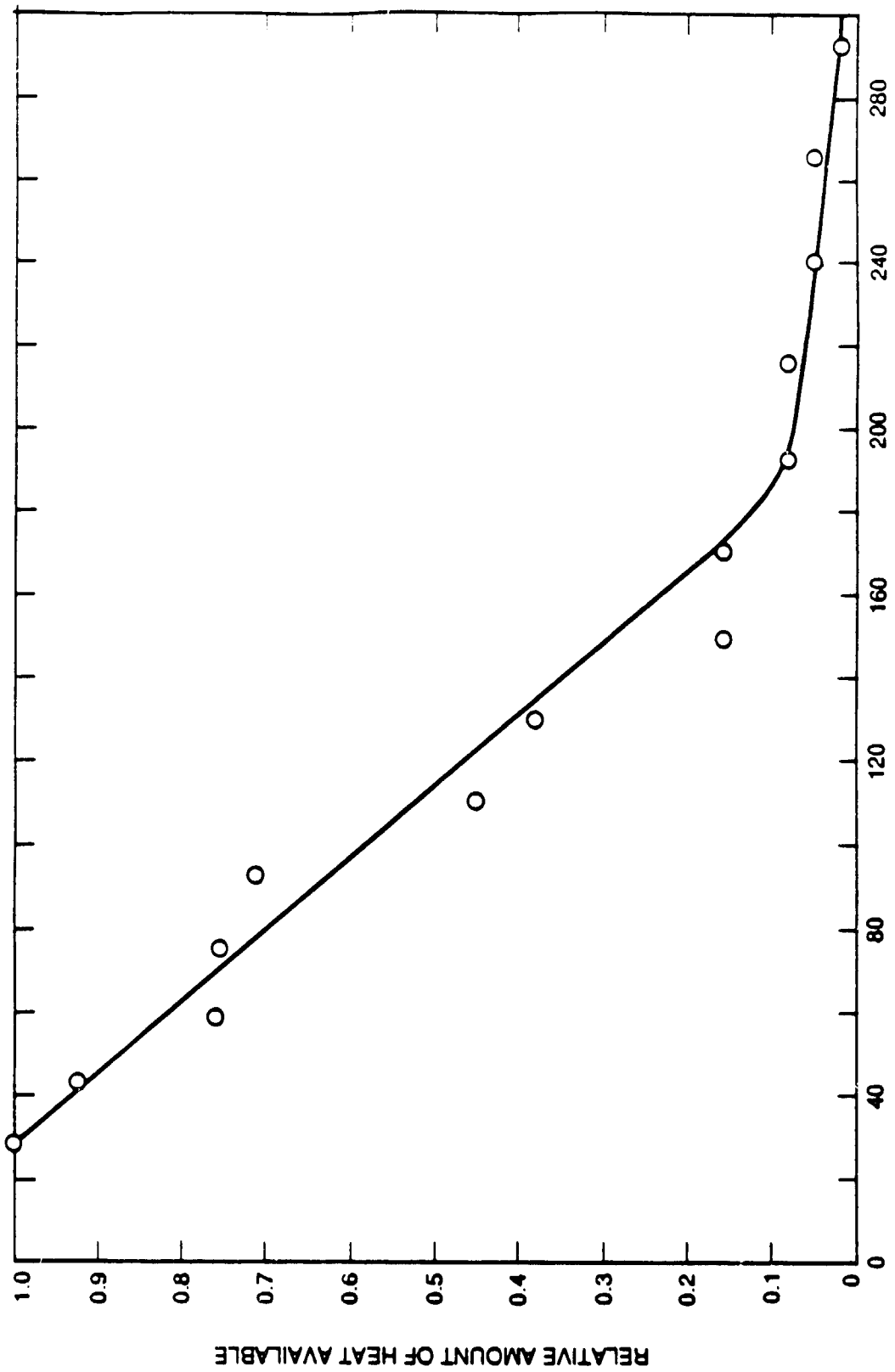

Figure 1. Relative Amounts of Energy Wasted in Industrial Streams vs. Stream Temperature

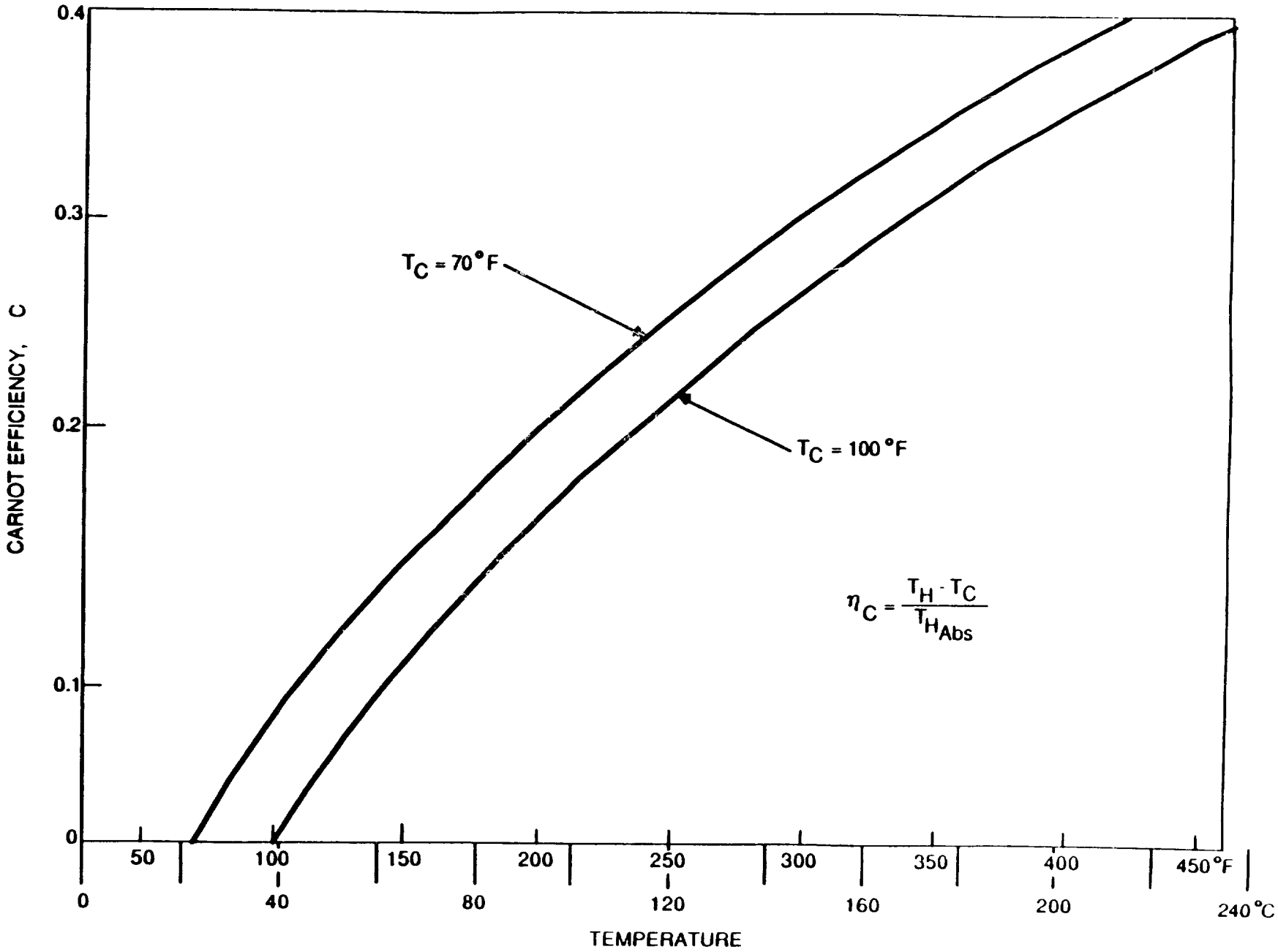

Figure 2. Carnot Efficiency vs. Temperature

CONCEPT	RESEARCH NEEDS	SYSTEM SCHEMATIC
• Alkali Metal Thermal-To-Electric Converter (AMTEC)	• Increased Electrode Power Density • Increased Electrode Lifetime • Performance Evaluation Based On Measured Parasitic Losses In A Recirculating Cell	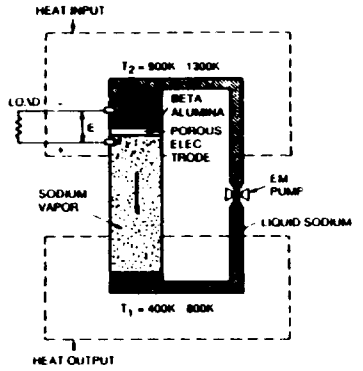
• Two-Phase Liquid-Metal MHD Generator (LMMHD)	• Reduced Slip Loss Between Gas Bubbles And Liquid Metal, i.e., Velocity Ratio Must Be Near Unity • Experimental Performance Verification	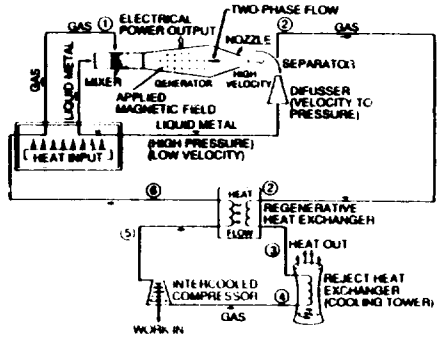

Figure 3. Alkali Metal (AMTEC) and Two-Phase Liquid Metal MHD (LMMHD) Thermal-to-Electric Conversion Systems.

CONCEPT	RESEARCH NEEDS	SYSTEM SCHEMATICS
• Thermoelectric	• Improved Efficiency • Materials With Higher Electric Conductivity And Lower Thermal Conductivity	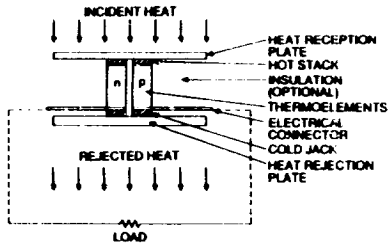
• Thermionic	• Improved Performance • Lower Temperature Operation • Control Of Oxygen In Cesium-Oxygen Vapor	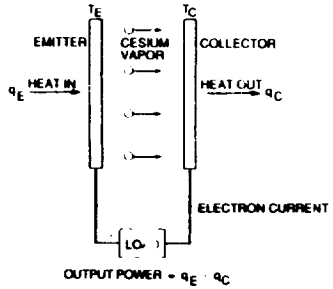
• Thermoelastic	• Concept For Converting Thermal-To-Electrical Energy Directly Without The Need Of A Conventional Shaft-Driven Generator Hook-up	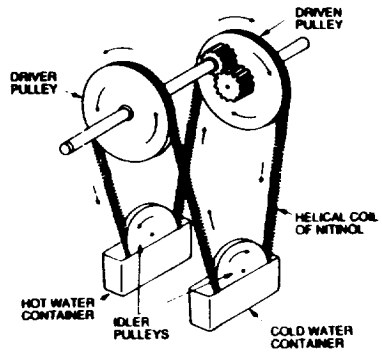

Figure 4. Thermoelectric, Thermionic, and Thermoelastic Energy Conversion Systems.

CONCEPT	RESEARCH NEEDS	SYSTEM SCHEMATICS
• Pyroelectric	• Materials With Higher Electrical Resistivity • Thermostatic Description • Evaluation of Hysteresis Losses • Determination Of New Thermodynamic Cycle Paths	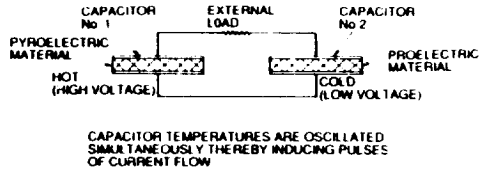
• Thermoacoustic	• Experimental Verification Of System Performance • Evaluation Of Working Fluids Other Than Sodium	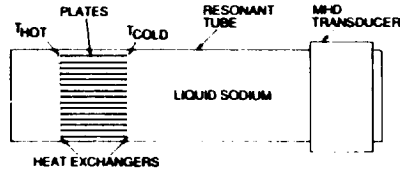
• Thermophotovoltaic	• Higher Temperature Semiconductor Materials • Increase In Efficiency Of Semiconductor Materials	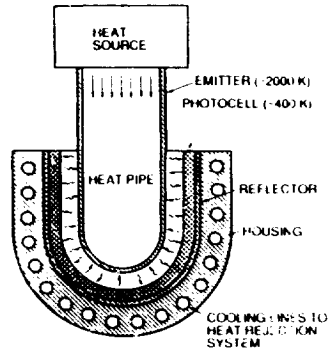

Figure 5. Pyroelectric, Thermoacoustic, and Thermophotovoltaic Direct Conversion Systems.

CONCEPT	RESEARCH NEEDS	SYSTEM SCHEMATIC
● Thermomagnetic Systems		
• Ferrohydrodynamic	• Determination Of Upper Bounds Of Magnetic Density For Ferrofluids • Experimental Verification Of Analyzed Thermodynamic Cycle Performance • Experimental Evaluation Of Losses	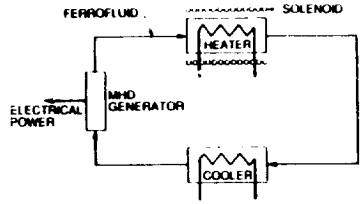
• Rotary	• Practical Optimized Matching Of Magnetic Field Profile With Regeneration And Rotation	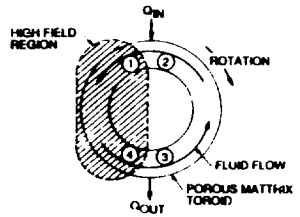
• Reciprocating	• Evaluation of Regeneration Process • Overall Performance Evaluation	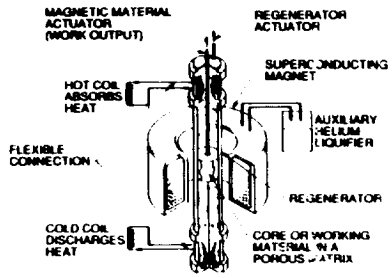

Figure 6. Thermomagnetic Energy Conversion Systems.

CONCEPT	RESEARCH NEEDS	SYSTEM SCHEMATIC
• Thermomagnetic Systems (contd)		
• Shunt	• Models Leading To Better Understanding • Experimental Verification Of Concept	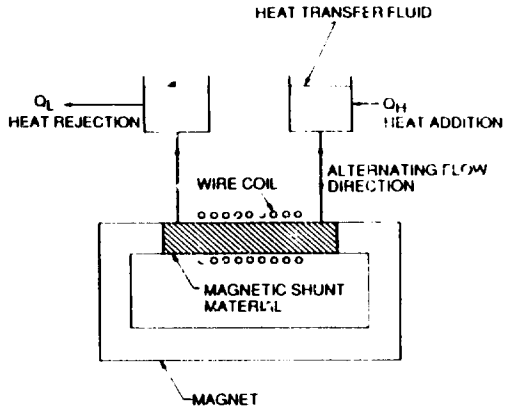
• Active Magnetic Regenerative Thermomagnetic Generator (AMRTG)	• A Computer Coded Model To Evaluate Performance And System Characteristics For Active And Passive Control Of The Applied Magnetic Field, And A Graded Curie Temperature • Experimental Evaluation Of Curie Temperature And Other Relevant Properties Of Ferromagnetic Materials Suitable As Working Substances For AMRTG's • Experimental Evaluation Of Performance If Modeling And Materials Investigations Indicate The Concept Promising	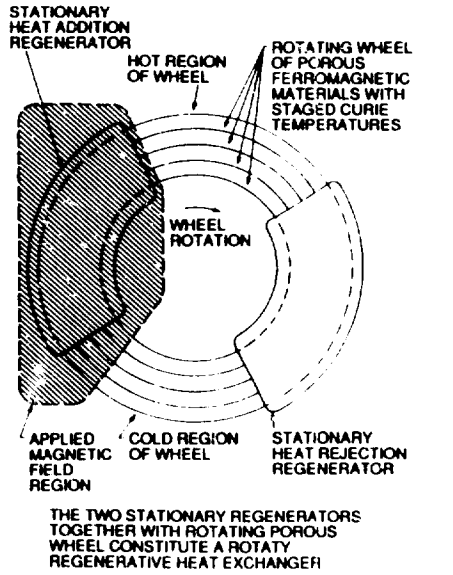

Figure 7. Additional Thermomagnetic Energy Conversion Systems.

CONCEPT	RESEARCH NEEDS	SYSTEM SCHEMATIC
• Combined Thermomagnetic And Pyroelectric Systems	• Analytical Assessment Of Performance Potential	TBD
	• Exploration Of Resonant Coupling Between The Inductor And The Capacitor With Energy Transfer Between A Magnetic Field And An Electric Field	

Figure 8. Combined Thermomagnetic and Pyroelectric Conversion Systems.

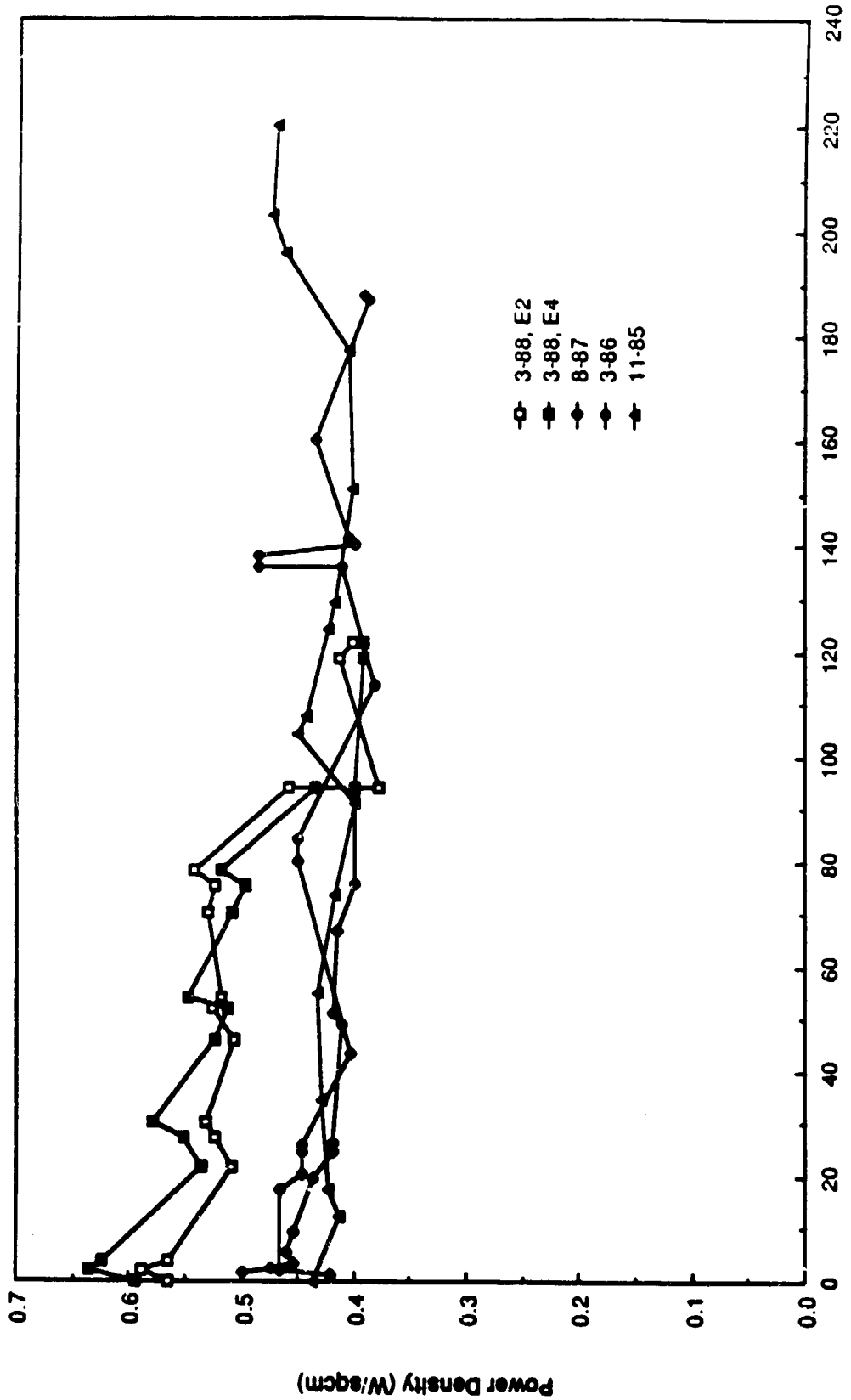

Figure 9. AMTEC: Maximum Power Density for Very Thin Molybdenum Electrodes

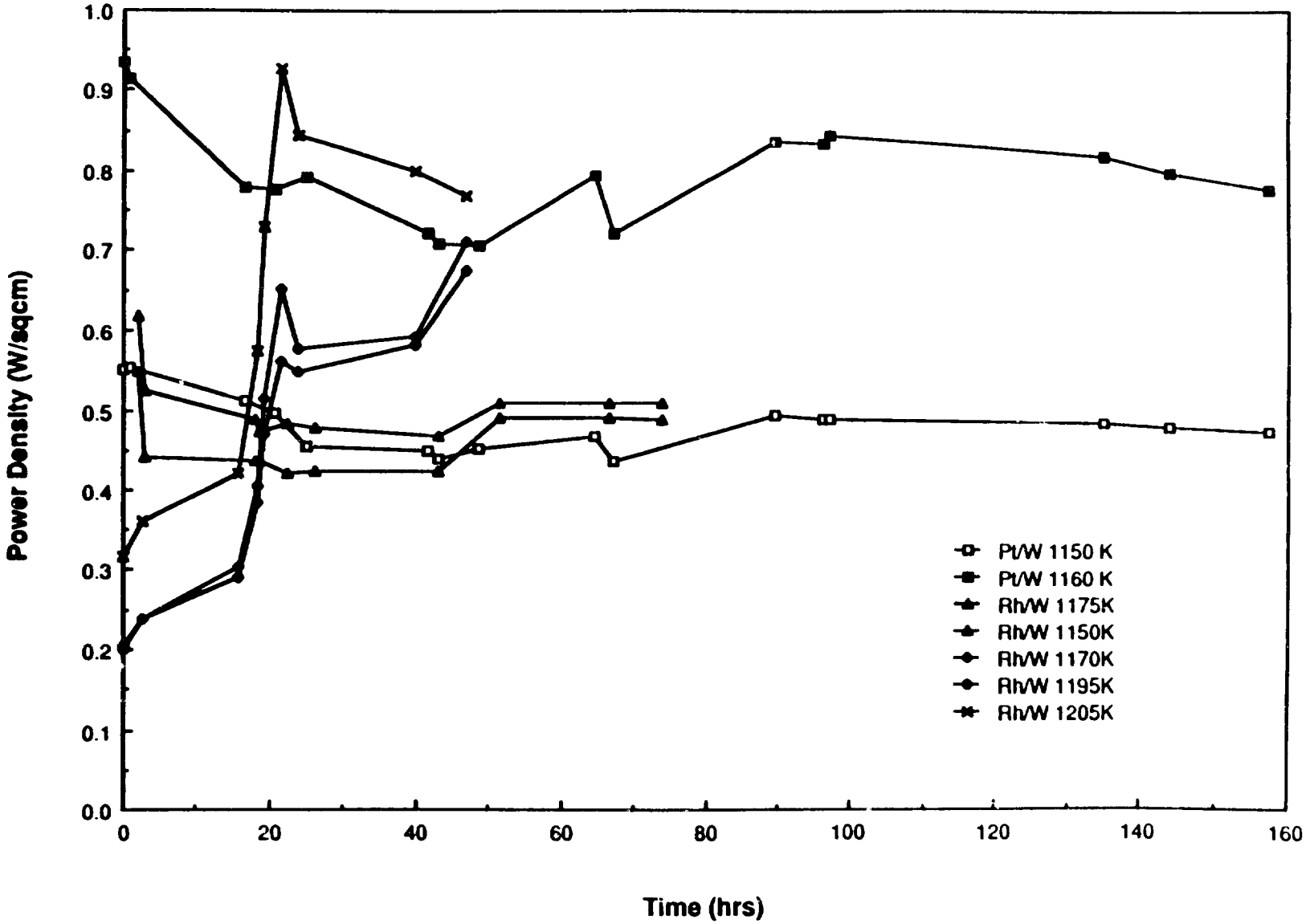

Figure 10. AMTEC: Maximum Power Density for Platinum/Tungsten and for Rhodium/Tungsten Electrodes

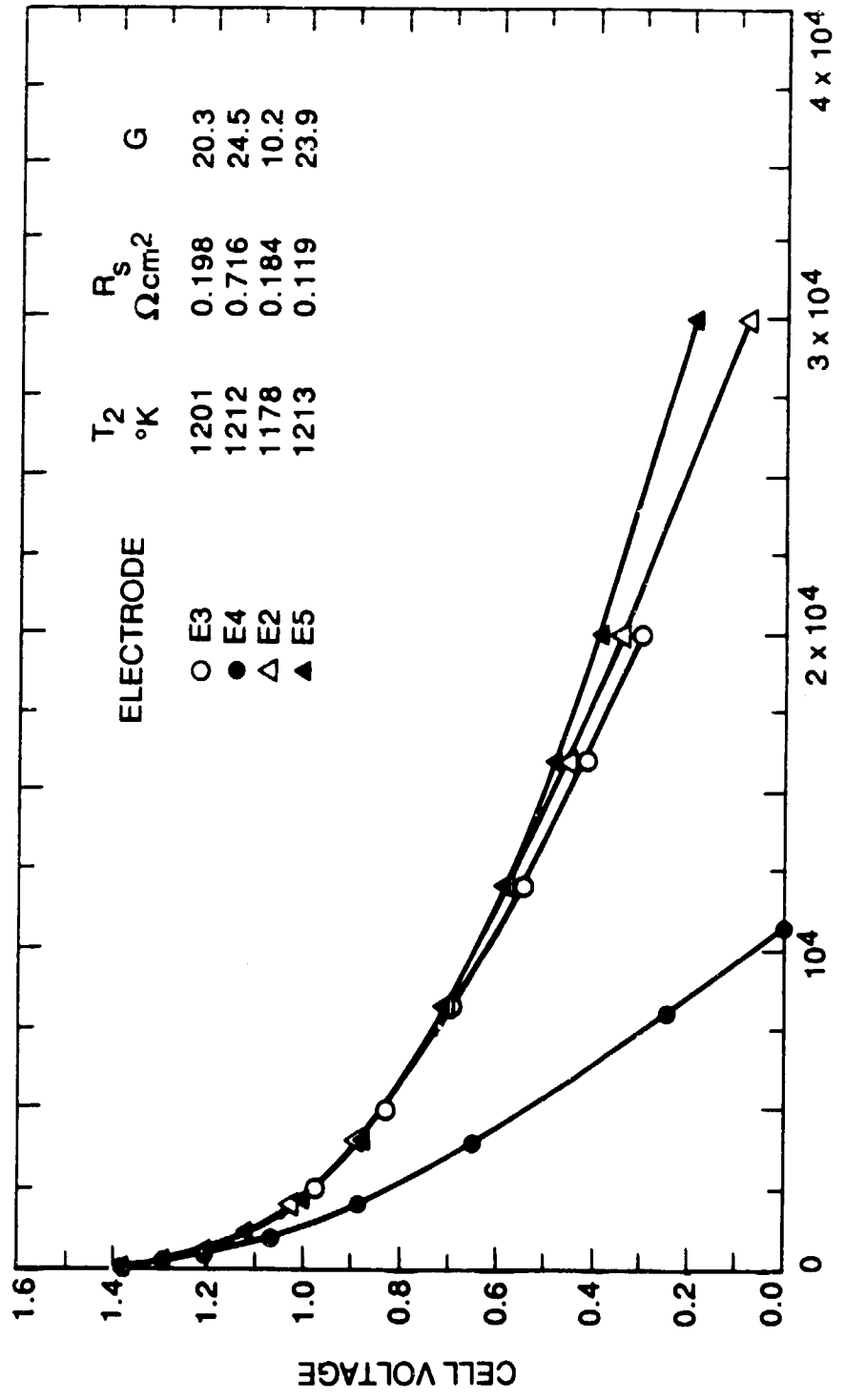

Figure 11. AMTEC: Rhodium/Tungsten Model Curves Fit to Data

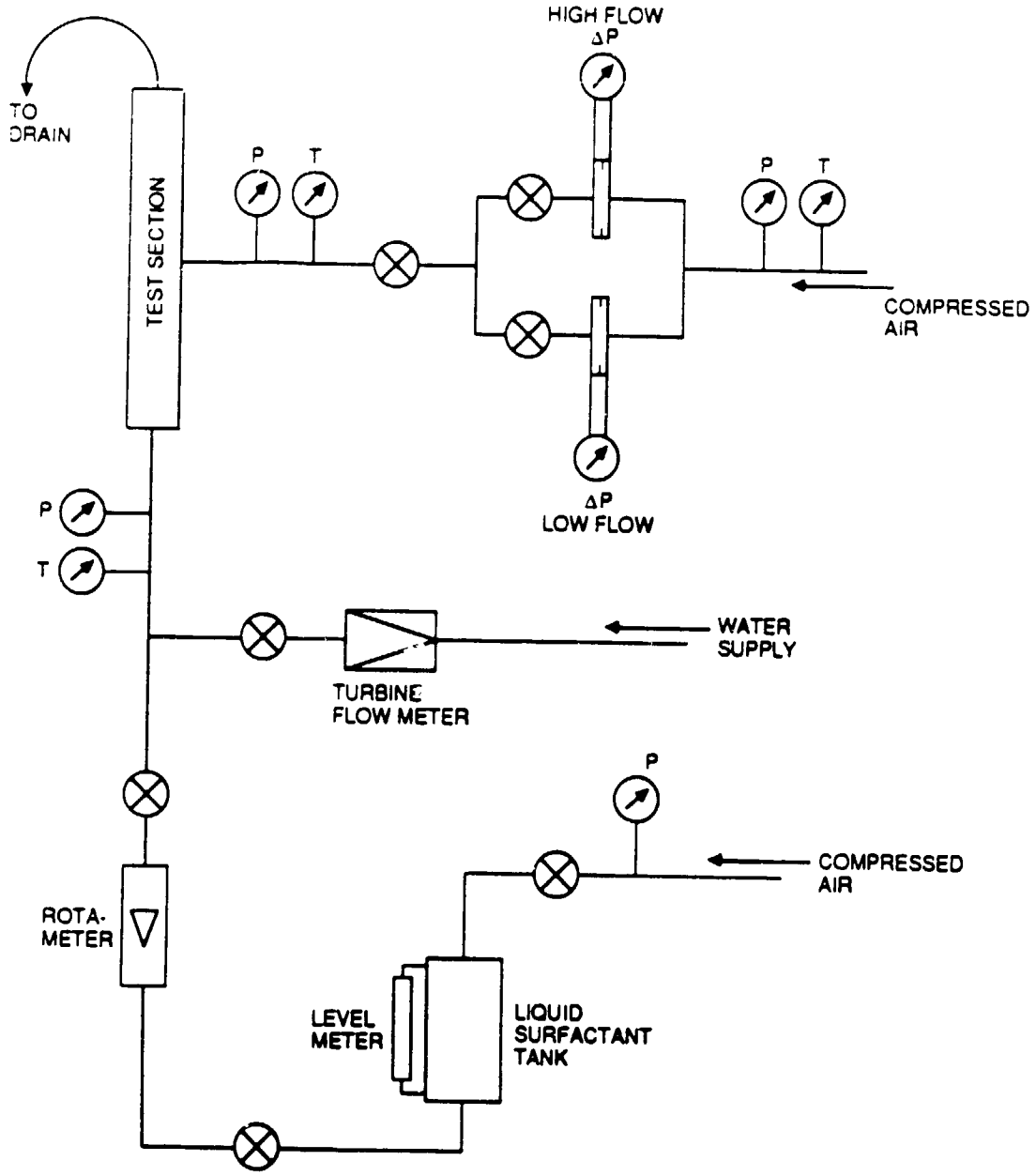

Figure 12. LMMHD: Schematic of the Flow System for Experiments of Air and Water Mixtures with the addition of Surface Active Agents

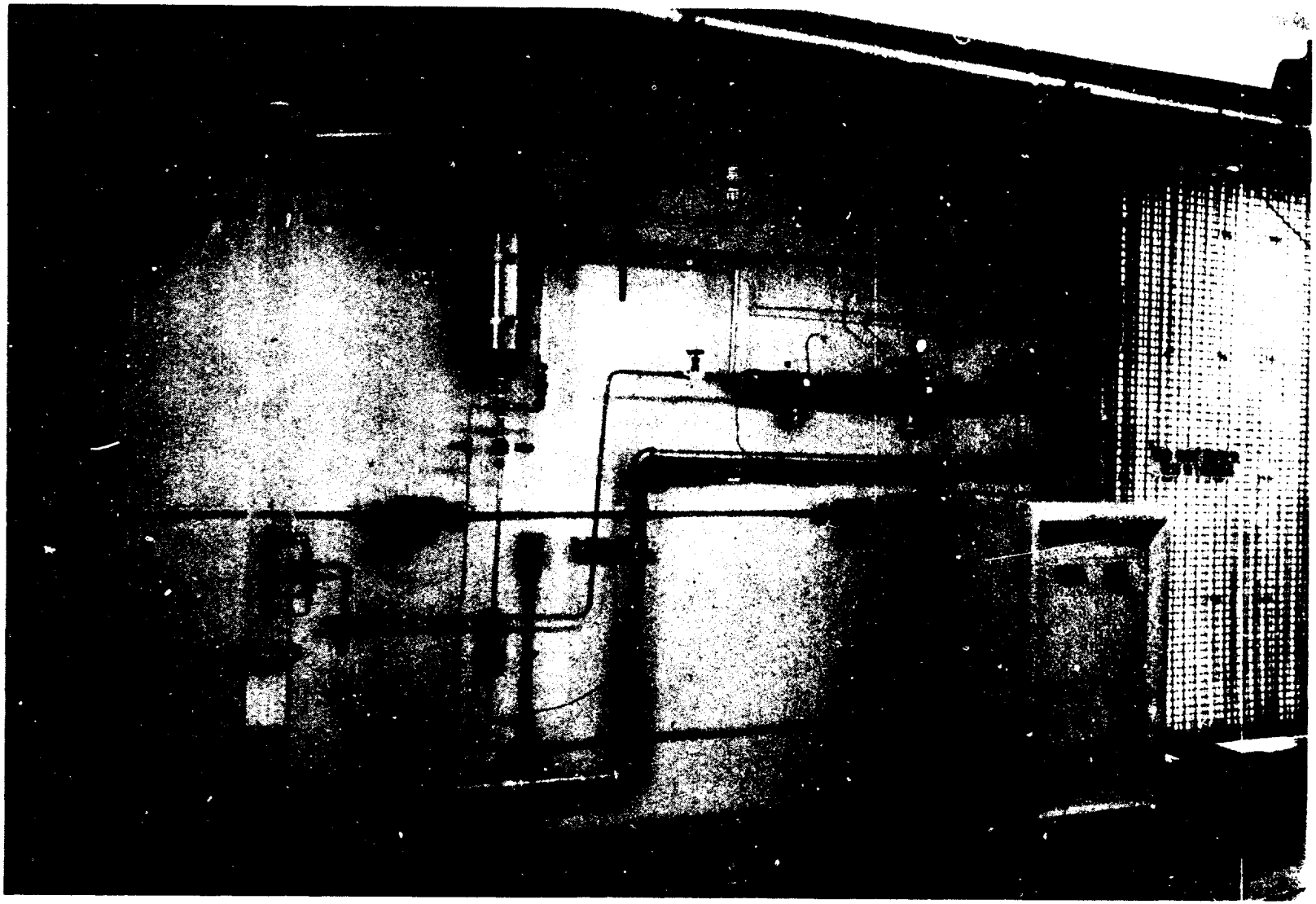

Figure 13. LMMHD: Photograph of the Air/Water Mixture Flow System

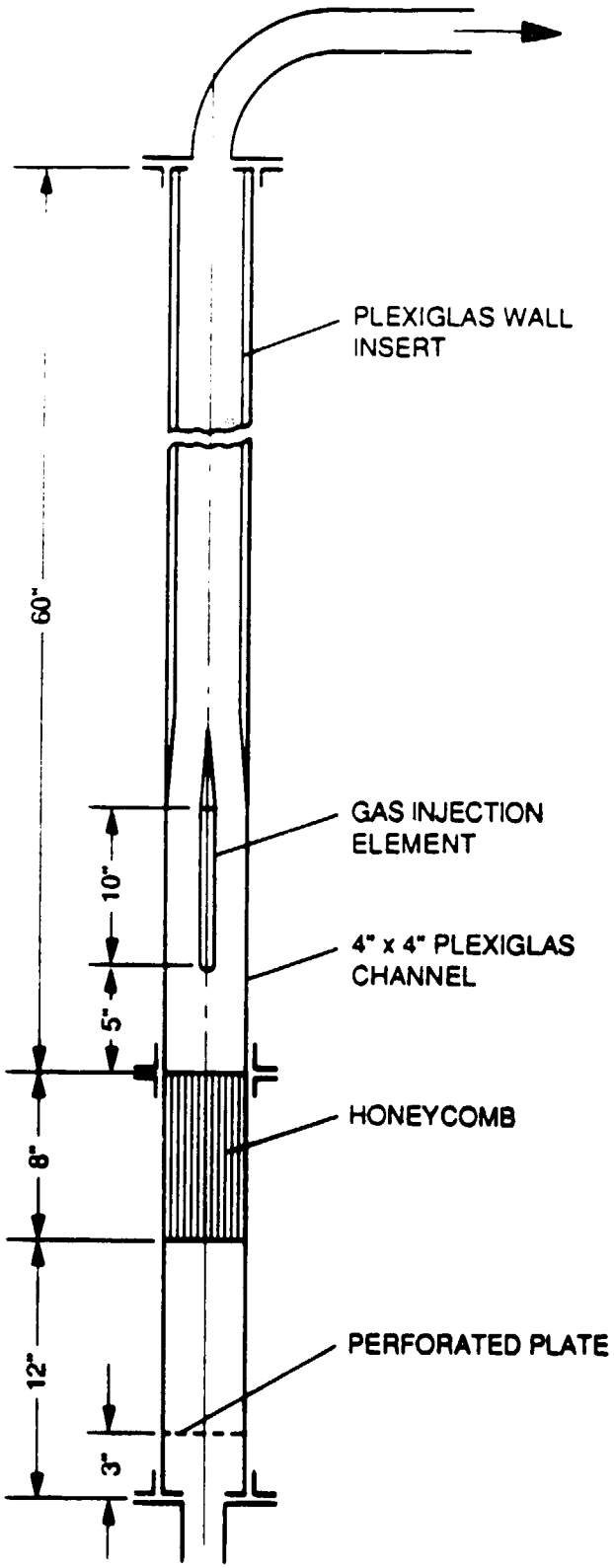

Figure 14. LMMHD: Details of the Transparent Test Section

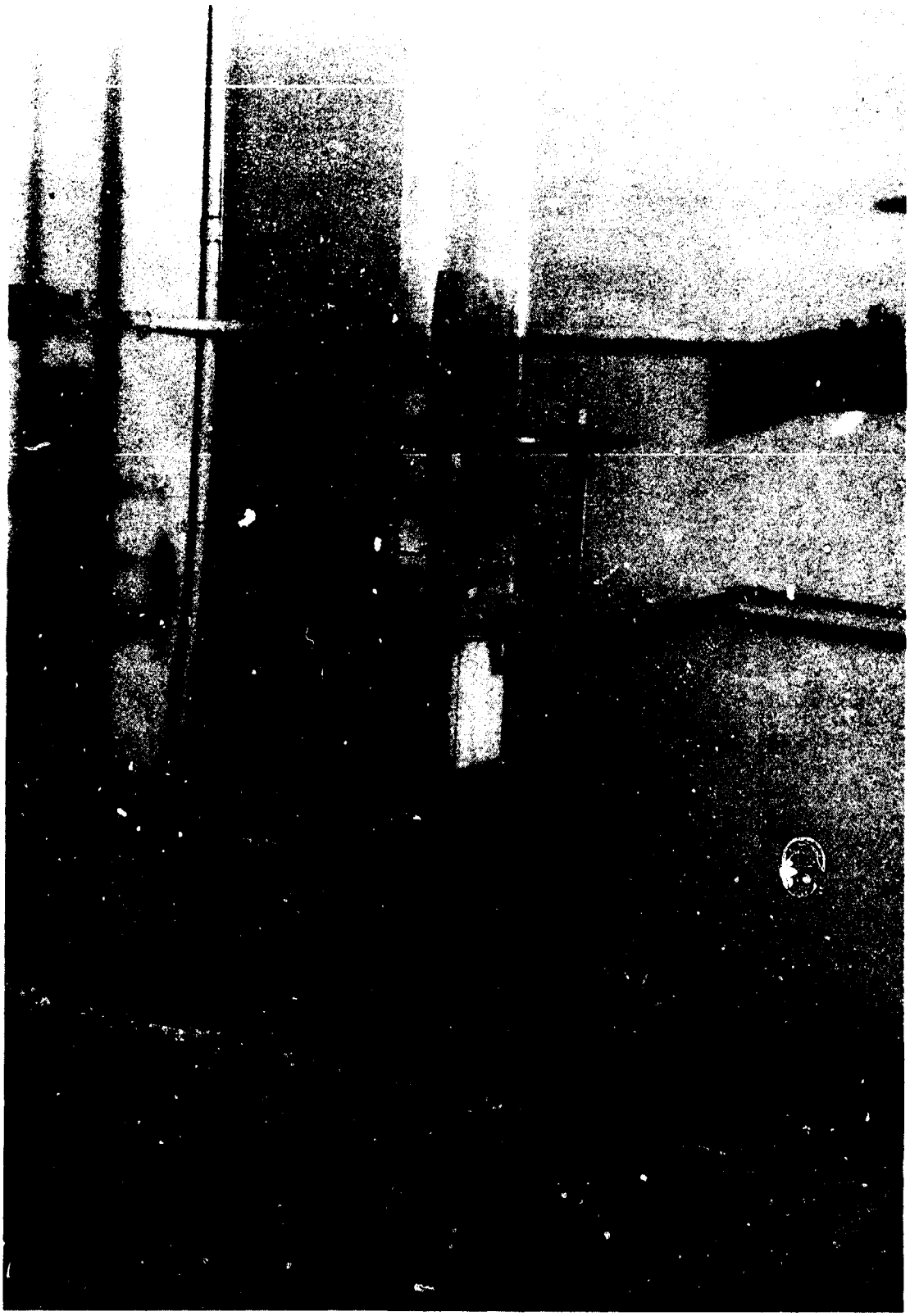

Figure 15. LMMHD: Photograph of the Lower Part of the Test Section Which Shows the Perforated Plate, Honeycomb, and Air Injection Element

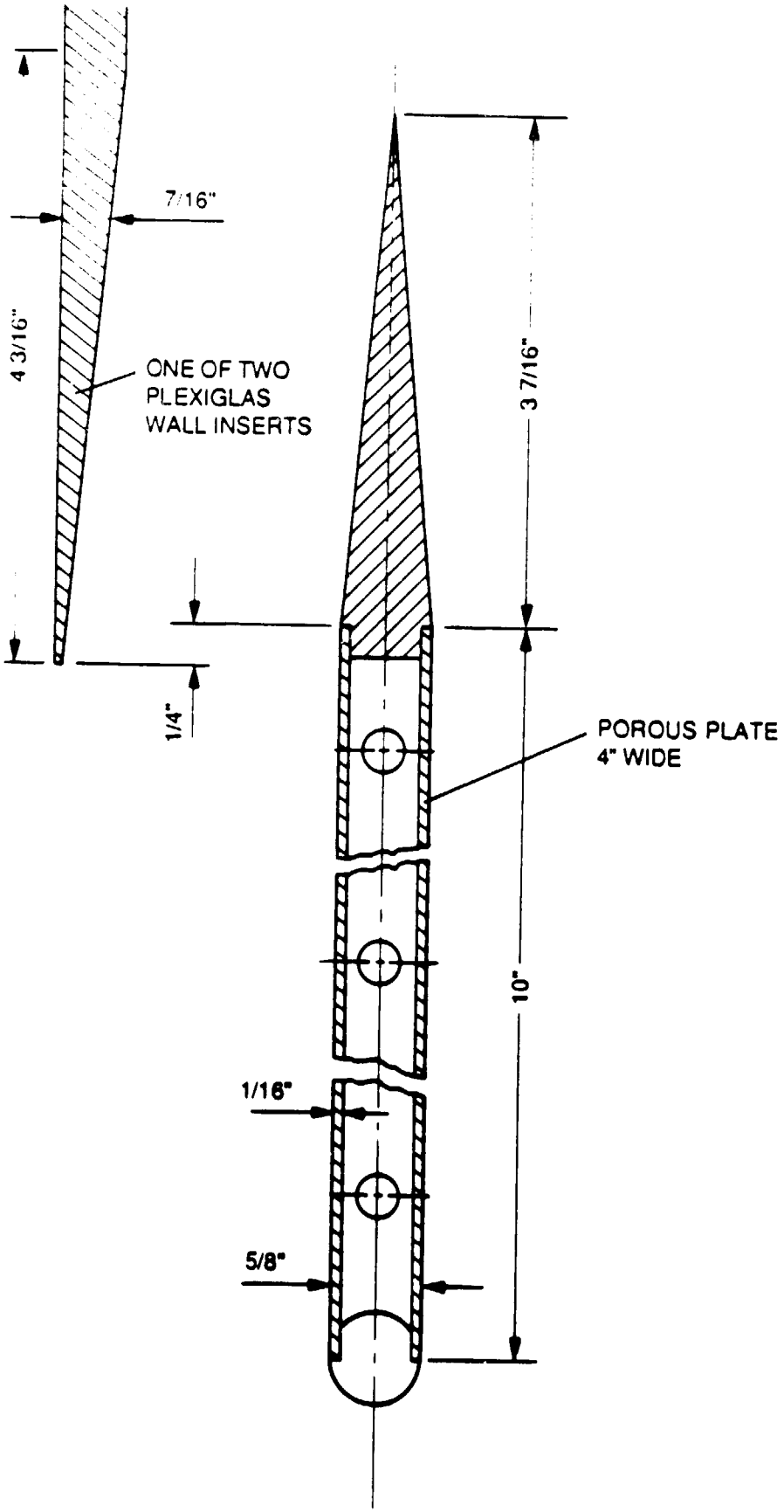

Figure 16. LMMHD: Details of the Air Injection Element

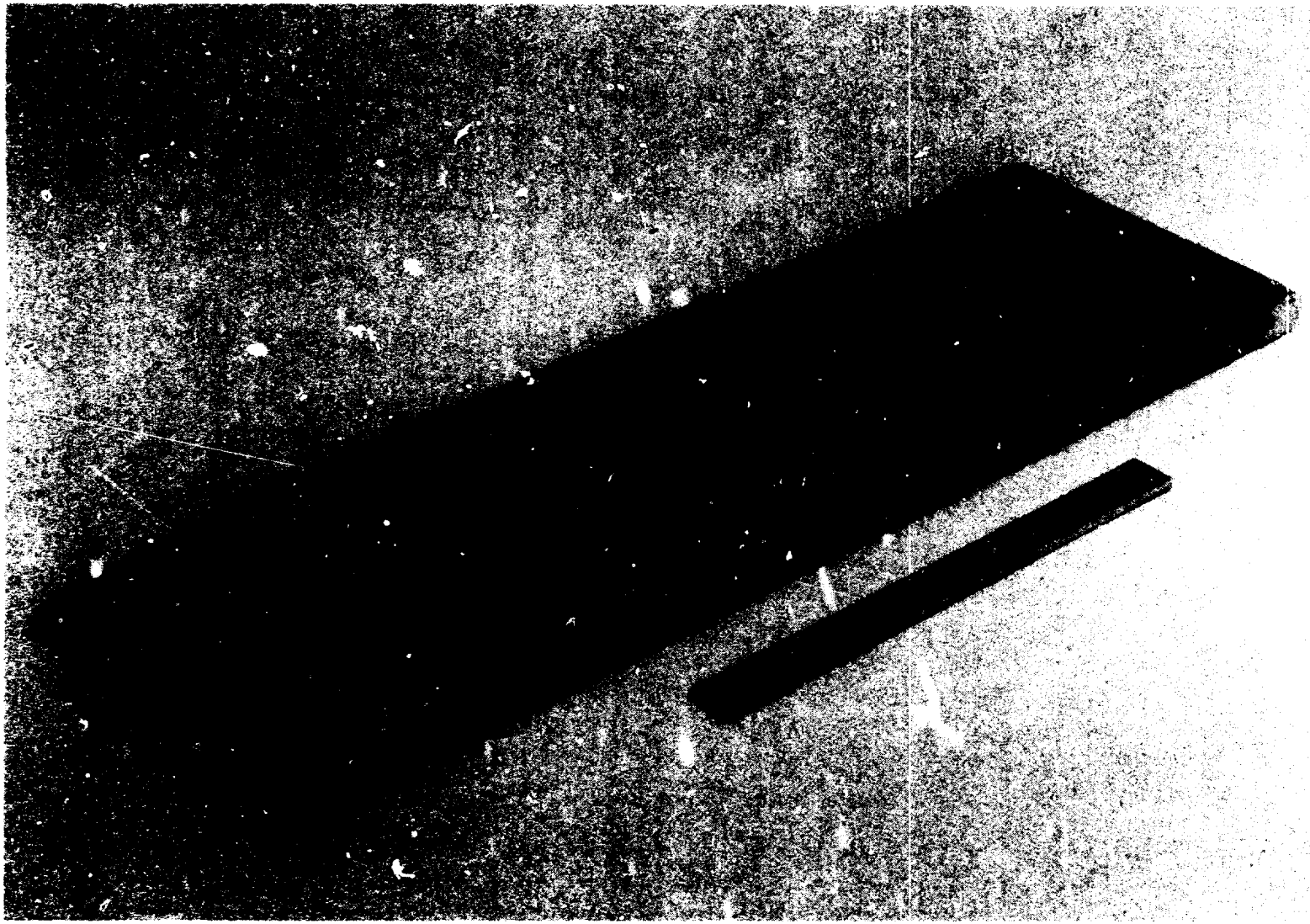

Figure 17. LMMHD: Photograph of the Air Injection Element

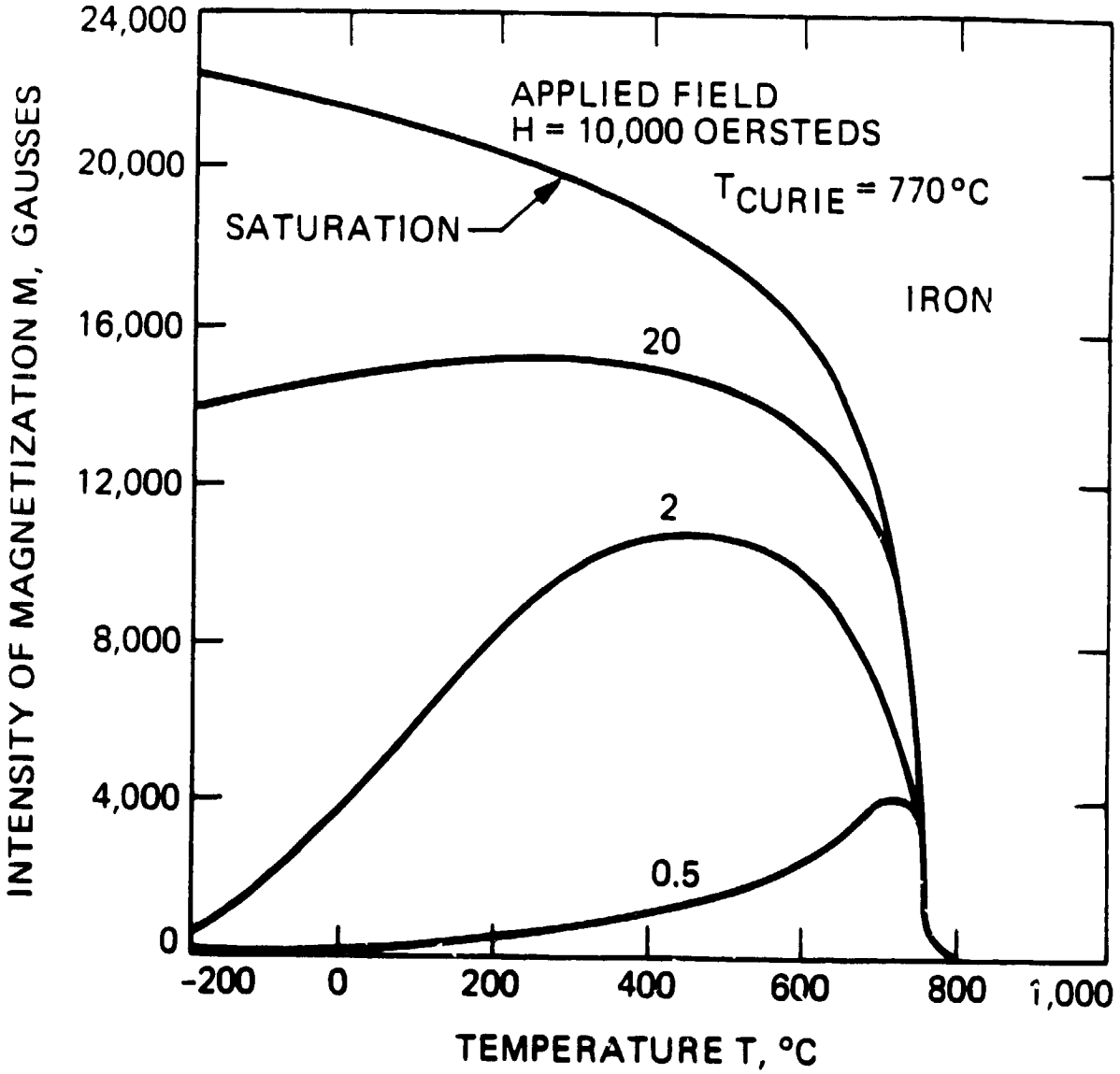

Figure 18. Effect of Temperature and Applied Magnetic Field on the Magnetization of Iron

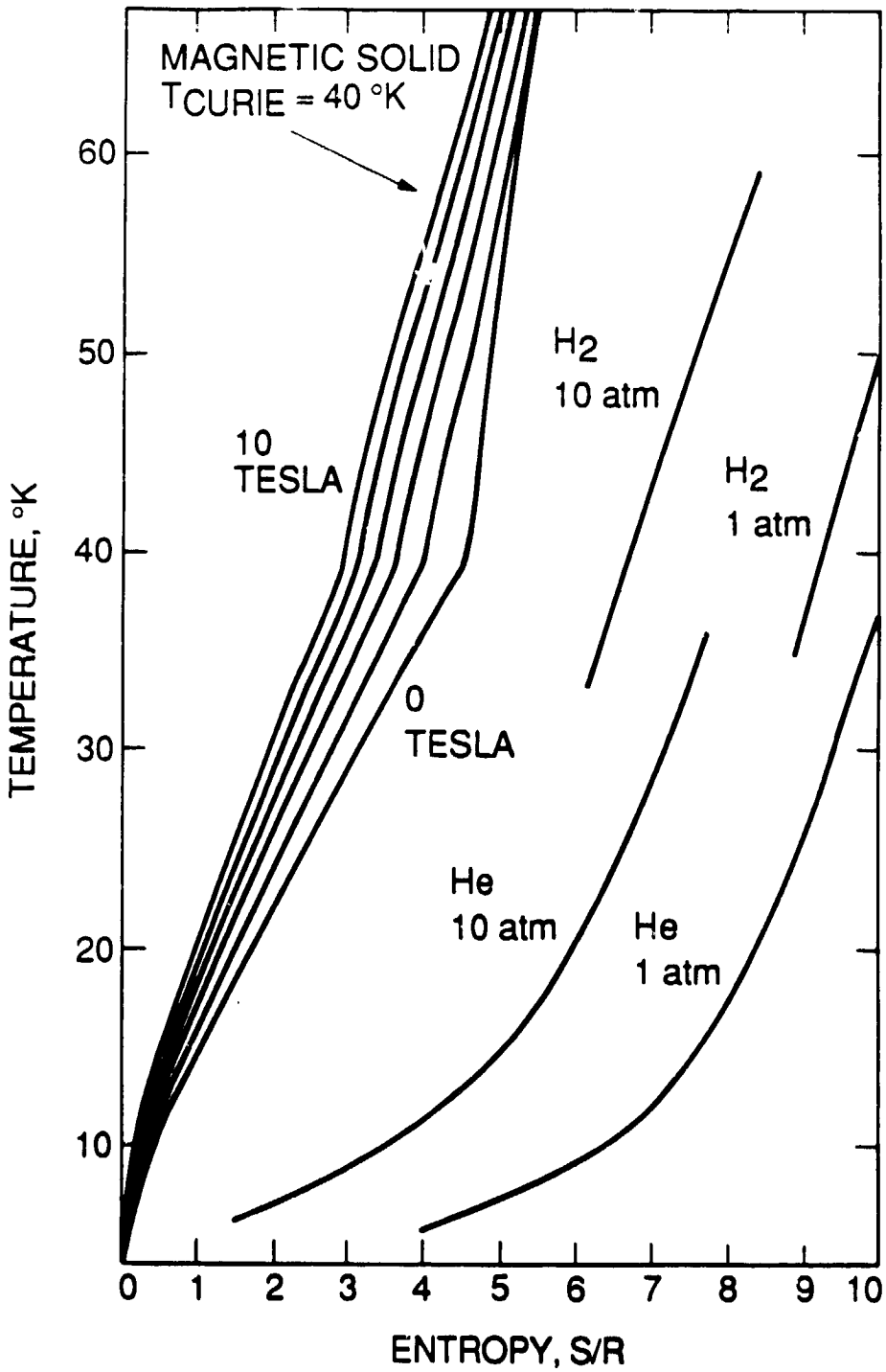

Figure 19. Temperature - Entropy Diagram for a Ferromagnetic Material with an applied Magnetic Field Between 0 and 10 Tesla, for Hydrogen Gas, and for Helium Gas.

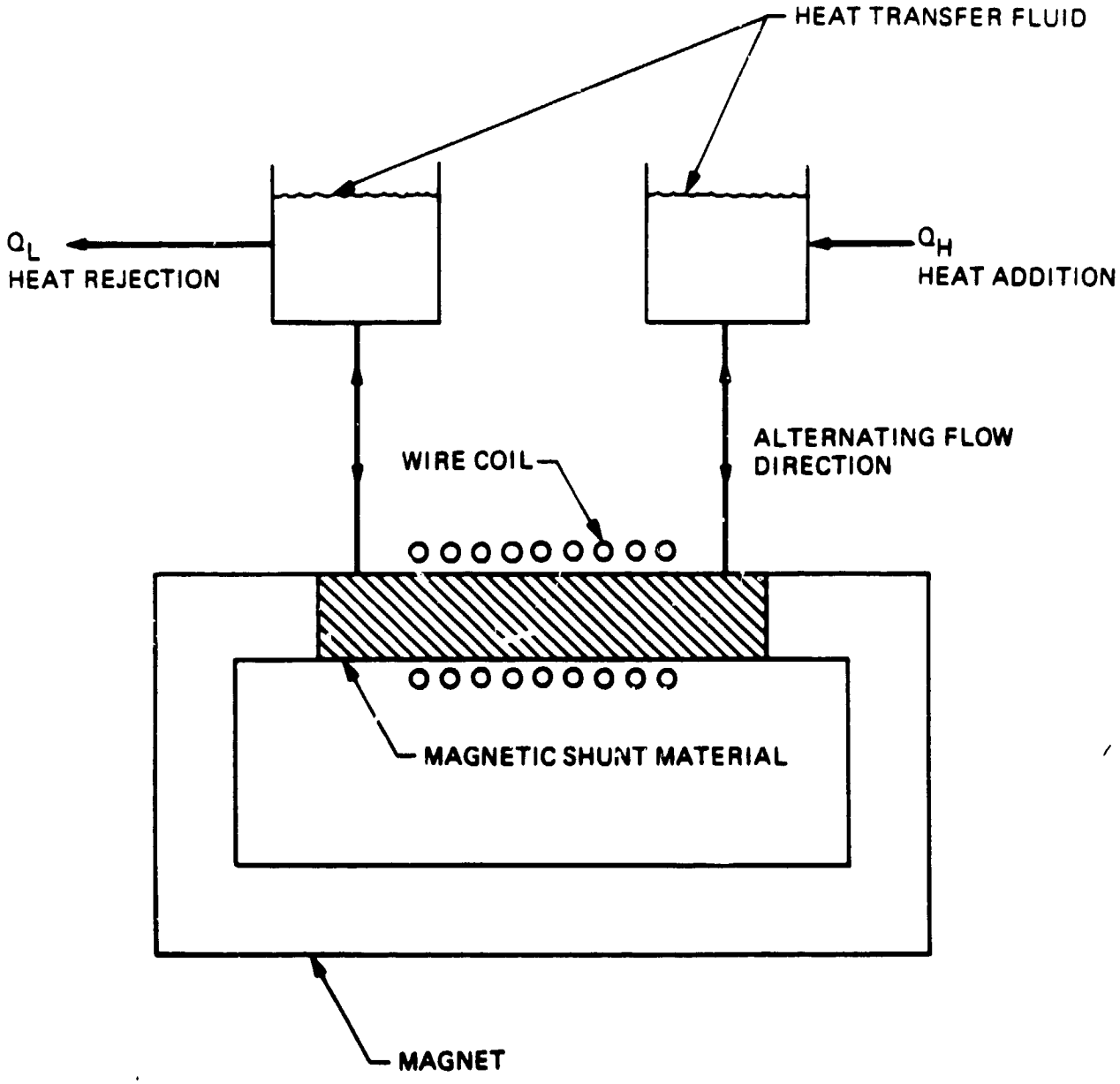

gure 20. Schematic Diagram of a Thermomagnetic Generator Concept in which a Ferromagnetic Shunt is Alternately Cooled and Heated

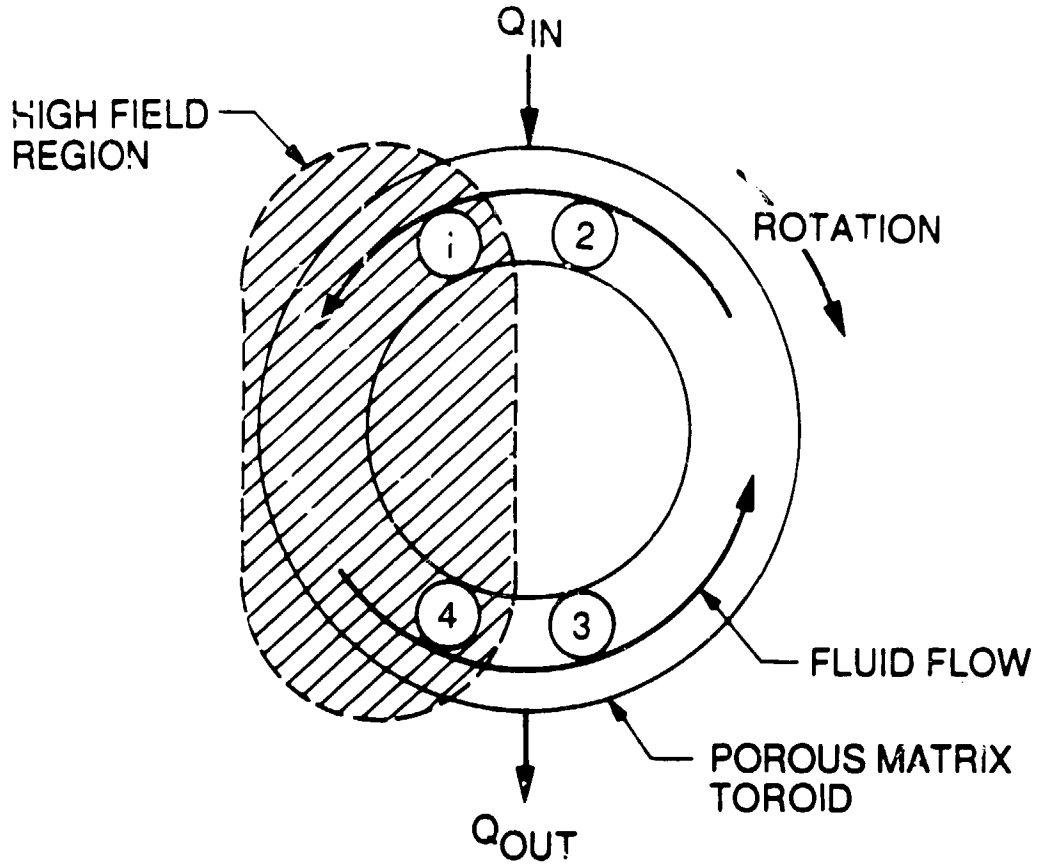

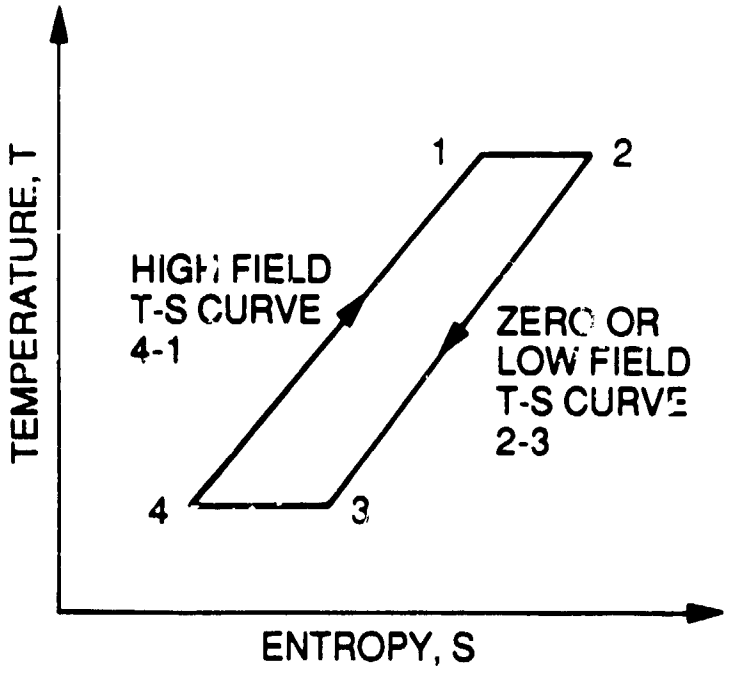

gure 21. A Regenerative Thermomagnetic Conversion Concept Consisting of a Solid Rotating Toroid with a Counterrotating Fluid, and the Associated Temperature - Entropy Diagram

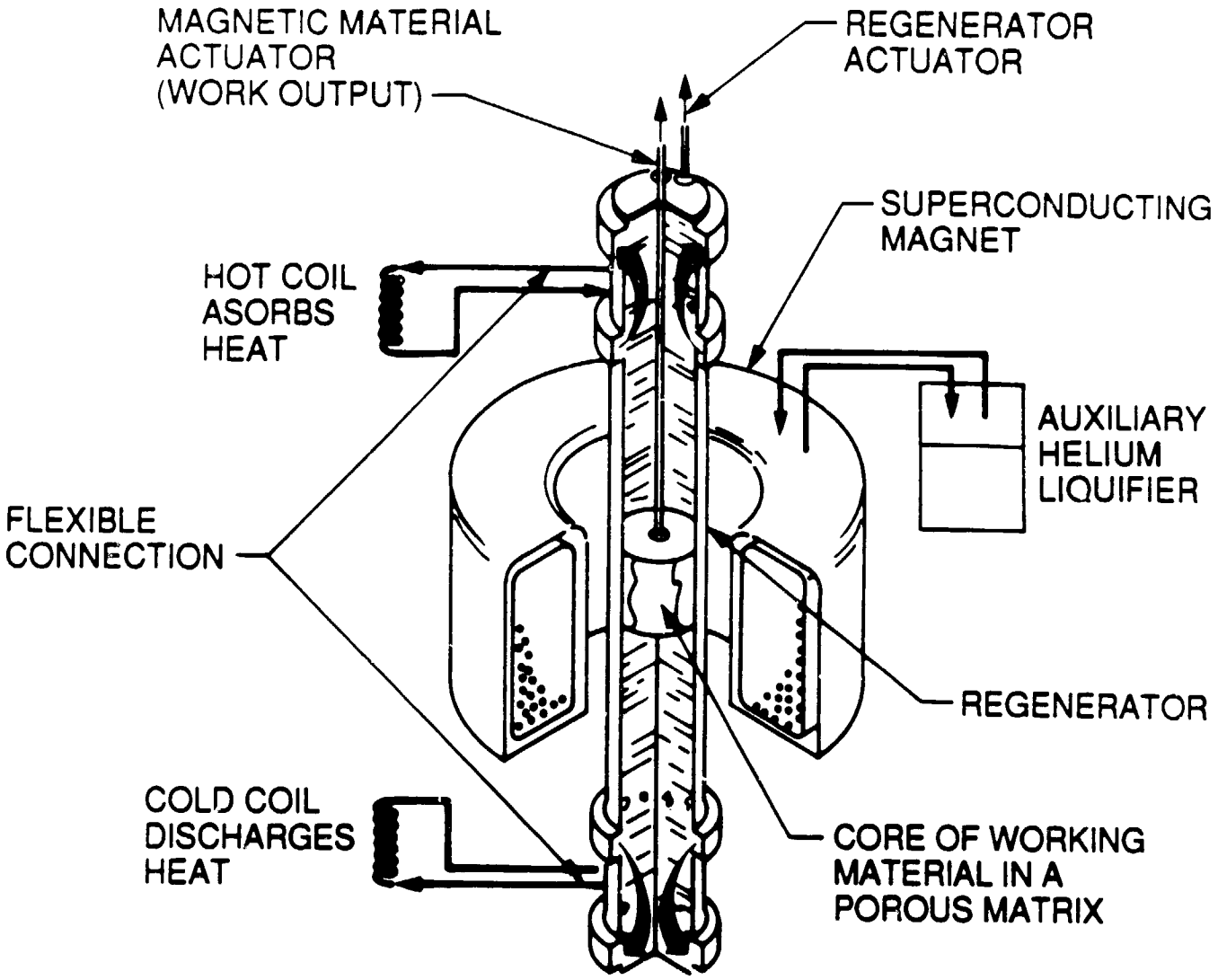

Figure 22. Reciprocating Type Thermomagnetic Generator

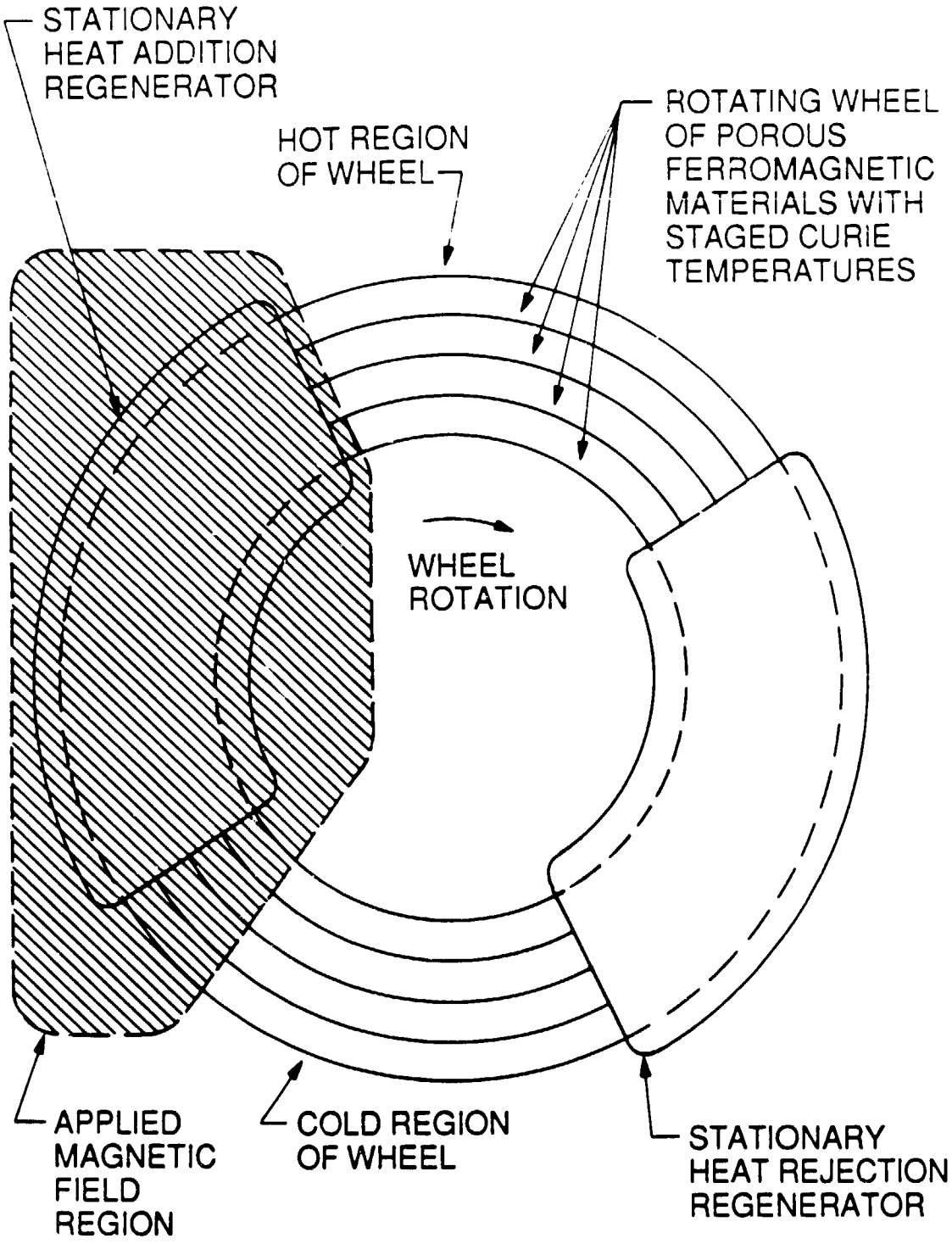

THE TWO STATIONARY REGENERATORS TOGETHER WITH THE ROTATING POROUS WHEEL CONSTITUTE A ROTARY REGENERATIVE HEAT EXCHANGER

Figure 23. Active Magnetic Regenerative Thermomagnetic Generator

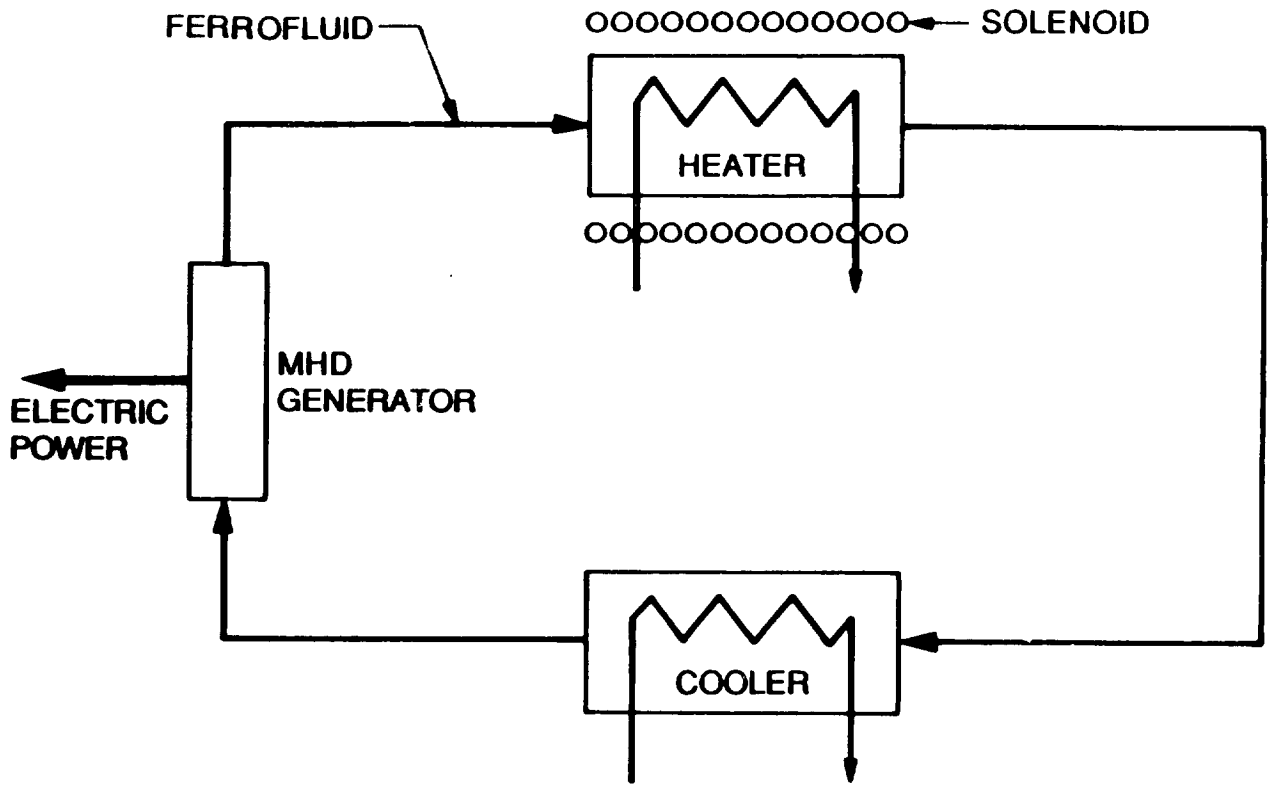

Figure 24. Schematic Diagram of a Simplified Thermomagnetic Converter using a Liquid Ferrohydrodynamic Material (Ferrofluid) as the working fluid

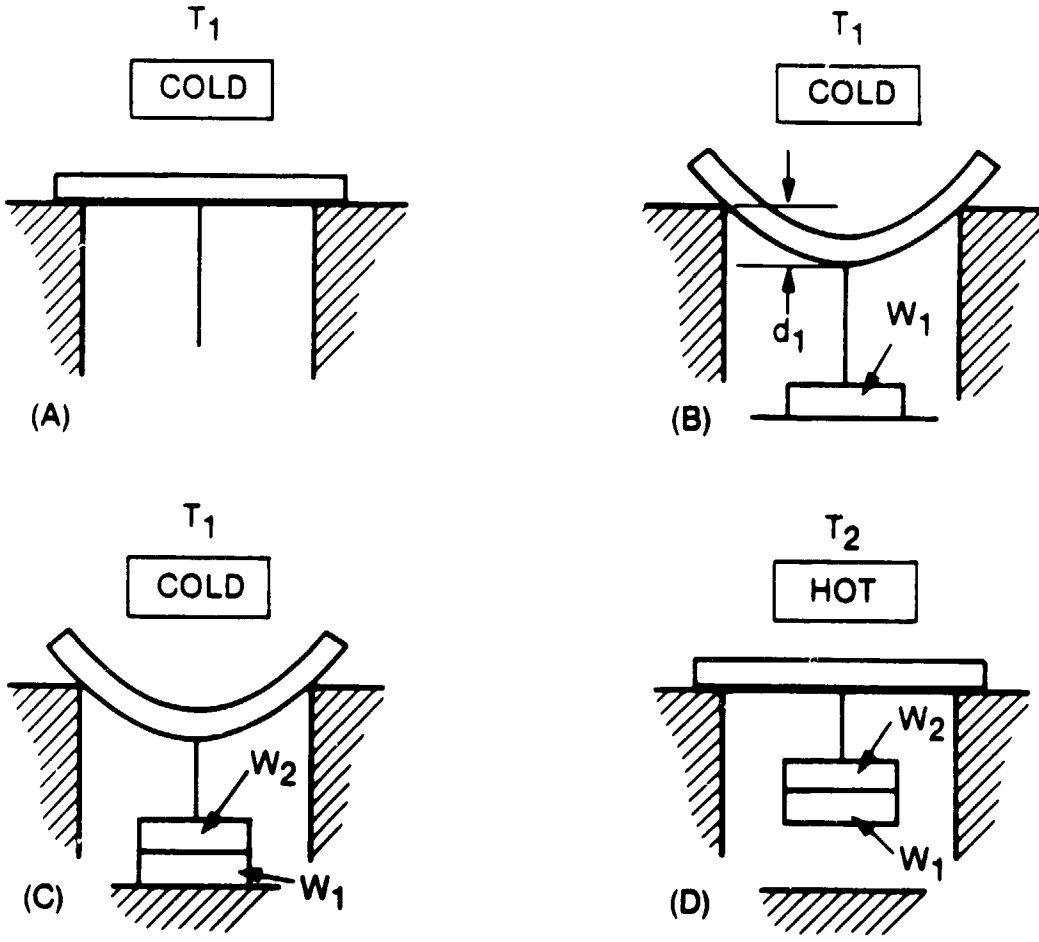

Figure 25. Conceptual Cycle for the operation of a Nitinol Heat Engine (Buehler and Goldstein) (A) Nitinol Element Memory Form at T_1; (B) Element Deformed at T_1, by Weight W_1; (C) Element subjected to Total Weight W_1+W_2 at T_1; (D) Element restored to original form at T_2 loaded with Weight W_1+W_2

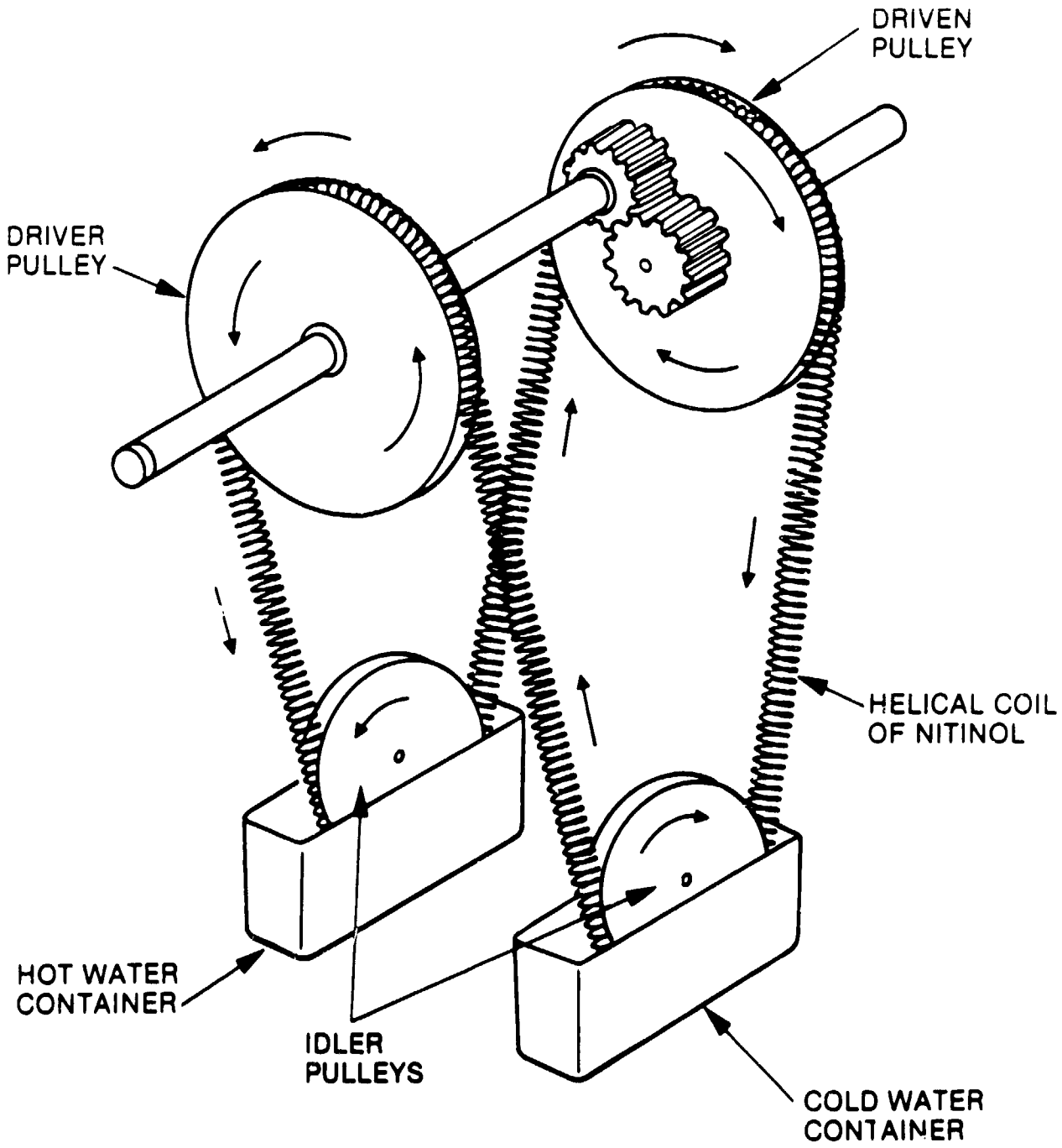

gure 26. Schematic of Gear-Coupled Turbine Engine driven by Helical Coil of Nitinol